

NATIONAL RADIO ASTRONOMY OBSERVATORY
Green Bank, West Virginia

July 24, 1972

TO: All Summer Students (and other derelicts)
FROM: E. B. Fomalont and G. S. Shostak
SUBJECT: Lecture notes for the Student Lectures on Radio Galaxies and
Quasars.

A detailed set of notes covering both lectures has been written by K. I. Kellermann and one copy will be placed in the Green Bank library and two copies in the Charlottesville library. They can be Xeroxed if you want a copy for yourself.

Short additional notes for the talk on quasars will be provided.

Summer Student Lecture Notes
Shostak & Fomalont

GALACTIC AND EXTRAGALACTIC RADIO ASTRONOMY

Chapter 12

Radio Galaxies and Quasars

K. I. Kellermann

Radio Galaxies and Quasars

Contents

- 12.1 Introduction
- 12.2 Radio Surveys
 - 12.2.1 3C and 3CR Surveys
 - 12.2.2 Parkes Survey
 - 12.2.3 Nomenclature
- 12.3 Optical Identification
 - 12.3.1 Types of Identification
 - 12.3.2 Radio Galaxies
 - 12.3.3 Quasars
- 12.4 Radio Properties
 - 12.4.1 Brightness Distribution
 - 12.4.2 Polarization
 - 12.4.3 Spectra
 - 12.4.4 Intensity Variations
 - 12.4.5 Empirical Relations
- 12.5 Theories of Radio Sources
 - 12.5.1 Synchrotron Emission
 - 12.5.2 Effect of Energy Losses
 - 12.5.3 Interpretation of Spectral Data
 - 12.5.4 Effect of Absorption by Ionized Hydrogen
 - 12.5.5 Synchrotron Self Absorption
 - 12.5.6 Inverse Compton Scattering
 - 12.5.7 Energy Considerations
 - 12.5.8 Interpretation of Time Variations
 - 12.5.9 Evolution of Radio Sources
- 12.6 Summary

12.1 INTRODUCTION

The discrete sources of radio emission were first distinguished from the general background radiation during the 1940's as a result of their rapid amplitude scintillations, and initially, it was thought that the scintillations were due to fluctuations in the intrinsic intensity of the discrete sources. Assuming that the dimensions of the sources could not greatly exceed the distance traveled by light during a typical fluctuation period of about 1 minute, it was concluded that the discrete sources were galactic stars located at relatively small distances from our solar system, and the term "radio star" was often used in referring to these sources.

The identification of two of the strongest sources, Virgo A and Centaurus A, with the nearby galaxies M87 and NGC 5128 by Bolton, Stanley and Slee in 1949 made it clear that at least some of the discrete sources were of extra galactic origin. In 1954 an accurate position measurement of the strong source Cygnus A led to the identification of this source with a relatively faint 15th magnitude galaxy having a red shift $z \approx 0.06$, (Baade and Minkowski, 1954) and the extragalactic nature of the discrete sources was generally recognized.

Although a few other radio sources were identified with galaxies during the 1950's, progress was slow due to the low accuracy of the radio source positions. By 1960, however, the positions of most of the strongest sources had been determined with an accuracy of about $10''$ arc and many were identified with various galaxy types. These galaxies, which are identified with strong radio sources, are generally referred to as "radio galaxies".

Most of the radio galaxies have bright emission lines, and so their red shift may be relatively easily determined. The faintest and most distant identified radio galaxy is the relatively strong radio source 3C 295 which has a red shift of 0.46 and an apparent magnitude of about 20.5. This identification, which was made in 1960, was the result of accurate radio positions determined at Caltech and at Cambridge, and stimulated the search for even more distant galaxies.

Continued efforts to identify galaxies were concentrated toward small diameter high surface brightness sources on the reasonable assumption that these were most easily observed at a large distance. A primary candidate was 3C 48 which had an angular size less than 1" arc, and was at the time the smallest strong source known. Accurate position measurements made in 1961 resulted what appeared to be unique identification with a 16th mag. stellar-object having a faint red wisp extending away from it. The absence of any other optical visible object near the radio source and the later discovery of significant night-to-night variations in light intensity lead to the reasonable conclusion that 3C 48, unlike other radio sources, was a true radio star. Soon two other relatively strong sources, 3C 286 and 3C 196 were also identified with "stars", and it appeared that more than 20% of all sources were of this class. The optical and radio properties were surprisingly dissimilar for the three objects and there were no unique radio properties to separate them from radio galaxies.

Early efforts at interpreting the emission line spectrum of 3C 48 were relatively unsuccessful, although the possibility of a large red shift was apparently considered. By 1962 most of the lines were thought to be identified with highly excited states of rare elements.

The identification of 3C 273 with a similar stellar object however, again

created doubt on the galactic interpretation which by 1963 was widely accepted. 3C 273 was tentively identified in Australia with a 13th mag star from a moderately accurate position determined with the 210' telescope. The position and identification were confirmed by a series of lunar occultations. These showed that the radio source was double, with one component being within 1" of the optical image, while the other component was elongated and coincident with a jet-like extension to the star. The identification was beyond question, although one wonders why it had not been made much earlier as 3C 273 was the brightest then unidentified source, of small angular size and located in an unconfused region of the sky near the galactic pole.

The optical spectrum of 3C 273 showed a series of bright emission lines which could only be identified with the Hydrogen Balmer series, but with a red shift of 0.16. This red shift was confirmed when the H γ line was found near the predicted wavelength of 7590 A $^{\circ}$ in the near infra-red. Adopting this red shift of 0.16 then led to the identification of the Mg II lines appearing at 3239 A $^{\circ}$.

A reinspection of the 3C 48 spectrum led to a red shift of 0.37 if a strong feature at 3832 A $^{\circ}$ was identified with Mg II. Other lines could then be identified with OII, NeIII, and Ne V. Additional spectra taken of other similar sources led to the identification of C $_{III}$ at 1909 A $^{\circ}$. C $_{IV}$ at 1550 A $^{\circ}$ and finally L α permitting red shifts as great as 2.8 to be measured.

This hitherto unrecognized class of radio source is usually referred to as "quasi stellar radio sources", or "QSS", or for short "quasars". Following the identification of the first quasars it was realized that they all had a strong

UV excess, and the search for further quasar identifications was simplified by looking for a very blue object located at the position of radio sources. In fact, many such objects were found, which optically appear to be quasars, but are radio quiet. These were originally referred to as Blue Stellar Objects (BSO'), Quasi Stellar Galaxies (QSG), or Quasi Stellar Object (QSO). Today the word "quasar" is generally used to refer to the entire class of stellar-type objects with large apparent red shifts, while QSO, and QSS refer to radio quiet and radio active quasars respectively.

It is now widely accepted that the radio emission from both galaxies (including our own galaxy) and quasars are due to synchrotron emission from relativistic particles moving in weak magnetic fields. The amount of energy required in form of relativistic particles is, however, very great, and the source of energy and how it is converted into relativistic particles has been one of the outstanding problems of modern astrophysics. The remainder of this chapter is devoted to a description of the observed properties of radio galaxies and quasars, and how these are interpreted in terms of the synchrotron mechanism.

12.2 RADIO SURVEYS

Catalogues of discrete sources have been prepared from extensive surveys using instruments especially design for this purpose. Initially these surveys were made at relatively long wavelengths near one meter, but as techniques have improved at the shorter wavelengths the surveys have been extended to wavelengths as short as a few cm.

In order to isolate the discrete sources from the intense emission observed from the galactic background, most of the earlier surveys were made with inter-

ferometer systems, which are relatively insensitive to the distributed background emission (see Chapter 10).

Today, catalogues of sources are available based on surveys made between 10 MHz and 5 GHz. Some of the surveys, particularly those made at the longer wavelengths cover essentially the entire observable sky to source densities of about 10^3 ster^{-1} . Other instruments, intended mainly for cosmological studies have reached source densities of about 10^5 ster^{-1} over very restricted parts of the sky. New instruments just coming into operation will reach densities of 10^6 ster^{-1} .

Generally the surveys have produced approximate values for the position and flux density for the catalogued sources. These catalogues have then been used as the basis for subsequent more accurate measurements over a wide range of wavelengths of properties such as

- a) the angular position in the sky
- b) the radio brightness distribution
- c) the radio frequency spectrum
- d) the amount and direction of any polarization and its angular distribution
- e) the time dependence of the radio emission.

A useful summary of radio source surveys has been compiled by Dixon () and contains the results of many separate surveys. The two most widely used catalogues are based on the Cambridge 3C and 3CR surveys, and the Parkes survey, which contain between them the great majority of sources which have been studied in detail for which optical data is available.
and

12.2.1 3C and 3CR Surveys - The 3CR catalogue (Bennet 1962) is based on the original 3C survey (Edge et. al. 1960) made at Cambridge at 159 MHz using a complex interferometer system. This survey was preceded by the 2C survey made with the same instrument at 81 MHz with a resolution two times poorer in each coordinate. The 2C catalogue contained 1936 sources, but due to the poor resolving power it became clear at an early stage that many of these sources were not real, and were due to blends of two or more sources in the primary antenna beam. Moreover, except for the strongest sources the determination of the flux density and angular coordinates was poor. The 3C survey with twice the resolution contained only 471 sources and was considerably more reliable. Nevertheless because of the relatively poor primary resolving power, there were still large errors in the positions and flux densities. In particular, it was frequently uncertain in which lobe of the interference pattern a particular source was located and this introduced large positional uncertainties.

In order to reduce these uncertainties, an additional survey was made at 178 MHz using a large parabolic cylinder antenna. The narrow E-W beam of this antenna eliminated nearly all of the lobe ambiguities of the original 3C catalogue. The data from the two surveys was combined to form the then most reliable radio source catalogue - the Revised 3C or 3CR Catalogue.

The same parabolic cylinder antenna was later used together with a smaller movable antenna as an aperture synthesis instrument (see Chapter 10) to make a complete high resolution survey of the northern sky (the 4C survey) which contains about 2000 sources.

12.2.2 Parkes Survey - The most extensive survey of the southern hemisphere radio sources has been made with the 210 foot radio telescope near Parkes, Australia.

This survey was initially made at 408 MHz (75 cm), except for the region $20^\circ < \delta > 2$ which was surveyed at 635 MHz (50 cm). Each source detected in the 50 or 75 cm finding survey was then reobserved at 20 and 11 cm to obtain more accurate positions and flux densities at these wavelengths. The Parkes Survey essentially replaces an earlier survey made at 86 MHz using a Mills Cross type antenna with a resolution of about $48'$ arc. Unlike the Cambridge 2C survey which was made about the same time and at nearly the same wavelength, the Mills Cross survey was mostly limited--not by inadequate resolution to separate nearby sources--but by low sensitivity. Nevertheless later work has shown that this survey was surprisingly accurate for its time, at least for the sources not near the limit of detection and this survey provides the only available data on the low frequency flux density of southern hemisphere sources.

12.2.3 Nomenclature - Most of the earlier surveys used a variety of complex schemes for naming and identifying sources. Unfortunately, the use of many names for a single source has led to needless confusion among workers. The recognition of this problem has led to the growing use of a system first used in the Parkes catalogue. In this system, each source is identified by a name of the form HHMM \pm DD, where HHMM represent the hours and minutes of right ascension, and \pm DD the degrees of declination prefixed by the sign. In order to preserve the identity of the observatory, the catalogue name is frequently preceded by a symbol identifying the observatory. Some prefixes in common use are PKS (Parkes), DW (Dwingeloo), B (Bologna), G (Green Bank), A (Arecibo). Often additional symbols are used to identify a particular survey.

12.3 Optical Identifications

Of the thousands of sources which have been catalogued only a few hundred have been reliably optically identified. Of these, roughly 70% are radio galaxies and 30% are quasars, although the exact fraction depends on the survey wavelength. For a considerable number of sources, accurate positions have been measured, and no optical object is found above the plate limit of the Palomar Sky Survey. For a much larger number of sources, the position accuracy is not sufficient to distinguish between the two or more objects lying within the error rectangle.

Optical identifications are important for two reasons.

- 1) It is not possible from radio measurements alone to determine the distance to a radio source. Thus, only if the radio source is identified with a galaxy or quasar, is it possible to measure the red shift and thus deduce the distance from the Hubble law. Distances are, of course, required to estimate the absolute radio luminosity and linear dimensions from measurements of radio flux density and angular size.
- 2) Optical studies of radio galaxies and quasars may give some insight into the problem of the origin of the intense radio emission.

For these reasons, much of the earlier work on the discrete radio sources was concentrated on the determination of accurate positions to permit unambiguous optical identifications. Today, coordinates of at least the stronger sources may be routinely determined by interferometry with an accuracy of the order of 1" arc. Nevertheless, the identifications are difficult. Firstly, often there is no apparent optical counterpart of the radio position, so that any associated

optical object is either subluminoous or at such a great distance, so that it is not visible to even the large optical telescopes. Secondly, many radio sources have dimensions of the order of 1" arc or more and a complex distribution of radio brightness so that more than one galaxy or quasar is found within the area covered by the source. Often, but not always, the identified galaxy lies at the centroid of radio emission, but it may also be coincident with one of the individual radio components, so that unambiguous identifications are difficult.

12.3.1 Types of Identifications - The identification of extragalactic radio sources are with a variety of objects as defined by Mathews, Morgan, and Schmidt (1964)

- a) normal spiral galaxies
- b) Seyfert galaxies
- c) E or Elliptical galaxies which are often the brightest member of a cluster.
- d) D galaxies, which are similar to Ellipticals but contain an extended halo.
- e) dB or Dumbell galaxies which contain a double nucleus imbedded in a common halo
- f) N galaxies which contain a compact nearly stellar nucleus
- g) QSO's or Quasi stellar objects (quasars)

The above sequence is very roughly in increasing order of absolute radio luminosity, although there is a wide spread of luminosity within each class.

In recent years, there has been a growing realization that the distinction between the various optical categories is largely subjective and may vary depending on the observer, the size of the telescope, and the distance of the

object. For example, the prototype quasar, 3C 48 is now sometimes classed as an N galaxy (eg. Morgan 1972). In another case, the optical jets from the quasar 3C 273 and the giant elliptical galaxy M87 show surprising similarity.

12.3.2 Radio Galaxies - Essentially all of the identified radio galaxies show moderate to strong narrow emission lines such as OIII at 372 \AA in their optical spectra, and this property has been used to confirm preliminary optical identifications based on the positional agreement of the radio source and the galaxy. Most of the identified galaxies are classed as giant ellipticals and have a surprisingly narrow dispersion in absolute optical magnitude of -20.8 ± 0.6 ($H = 100 \text{ km/sec/Mpc}$). Initially most of the identifications were with galaxies which showed some sort of optical peculiarity. For example, M87 (Virgo A) has a well known jet extending from its nucleus; NGC 5128 (Centaurus A) contains a conspicuous dark band across the galaxy; Cygnus A has a double nucleus with intense emission lines which was the basis for the idea that the radio emissions was the result of collisions between two galaxies. Other identifications were with Seyfert galaxies such as NGC 1068 and NGC 1275.

Although more recently many radio galaxies have been identified which show no obvious optical peculiarity, there has been some degree of bias toward accepting identification with galaxies which show some abnormality. Since the identification process is a very subjective one, involving not only positional coincidence but the size and structure of the radio source, as well as the presence of strong emission lines and optical features such as jets or dust, the significance of these phenomena on the radio emission is not clear without completing the difficult task of obtaining optical identifications of a complete sample of radio sources.

Because two of the early radio source identifications were with the Seyfert galaxies NGC 1068 and NGC 1275 it has been widely thought that the Seyfert phenomena is associated with intense radio emission. In fact, this is not the case, since none of the other well known Seyfert galaxies show radio emission much greater than the normal spiral galaxies. Moreover even NGC 1068 has a luminosity of only 10^{40} ergs/sec, only slightly greater than other spiral galaxies, and the classification of NGC 1275 as a Seyfert is now questioned by many astronomers. Although a few other radio sources have been identified with galaxies which were later classed as Seyferts, it appears in general that the radio luminosity of Seyfert galaxies does not significantly exceed that of normal spirals, and the fraction of Seyfert galaxies which are strong radio sources appears to be comparable with that of giant ellipticals.

Similarly, attempts to detect radio emission from other "peculiar" galaxies such as the Zwickey compact galaxies, Markarian galaxies, or the interacting galaxies catalogued by Arp and Vorontzov-Velyaminov have been for the most part unsuccessful, and contrary to widely held belief, there is no evidence that these "exotic" galaxies are likely to be strong radio sources.

Red shifts are available for only about 100 of the identified radio galaxies. These have absolute radio luminosities which range from about 10^{40} to 10^{45} ergs/sec. In contrast to the radio galaxies which were all identified as galaxies which are coincident with catalogued radio sources, are the so called "normal" galaxies. These are the optically bright galaxies from which weak radio emission has been detected as a result of a special search. The absolute radio luminosity of the "normal" galaxies is of the order of 10^{37} to 10^{38} ergs/sec that is comparable to the power radiated from our own galaxy.

Normal
G

It is not yet clear to what extent the normal galaxies are a separate phenomena or just an extension of the radio galaxy phenomena. In particular, it has not yet been definitely established whether the two groups form a continuous sequence of absolute radio luminosity, or whether the luminosity function has a minimum near $10^{39} - 10^{40}$ ergs/sec. More radio observations of faint galaxies and more identifications of weak radio sources are needed to fill in this gap in the radio luminosity function.

The identified quasars are all very strong radio sources with luminosities comparable to the most luminous radio galaxies. Of the quasars which were first located from optical measurements, only a few percent have been detected as radio sources. But considering the large red shifts, the upper limit to the radio luminosity of the undetected quasars is still large.

Searches for radio emission from rich clusters of galaxies have been more fruitful, although it appears that the radio emission originates in the brightest cluster member, and that cluster membership does not affect the probability of radio emission. About 5 to 10 percent of the giant elliptical galaxies which are the brightest cluster members show detectable radio emission (Rogstadt and Ekers, 1969).

There is some evidence the radio luminosity depends weakly on the optical luminosity for both galaxies and quasars. In the case of galaxies the strong radio sources almost all show bright emission lines.

12.3.3 Quasars - The optical properties of quasars may be summarized as follows:

- 1) They appear stellar on direct photographs, although in some cases there is a faint jet or wisp extending from the stellar object.

- 2) They have large red shifts ranging up to $z = 2.8$.
- 3) Assuming that the red shifts are cosmological and that the distance is given by the Hubble law with a Hubble constant, H equal to 100 km/sec/Mpc, then the absolute optical magnitudes range from -22 to -26 so that they are up to 100 times brighter than the most luminous galaxies at optical wavelengths.
- 4) Often the optical emission is variable on time scales ranging from a few hours to a few years.
- 5) The luminosity rises sharply toward the infra-red where most of the radiated energy lies. There is also an excess of UV emission compared with galaxies, so that the presence of a large red shift causes the quasar to appear blue when measured by UBV photometry or when the color is estimated from the "red" and "blue" plates of the Palomar Sky Survey.
- 6) The spectra show intense broad emission lines with line widths corresponding to velocities up to 4000 km/sec. The most commonly observed lines are those of $\text{Ly}\alpha$ ($\lambda 1216$), CIV ($\lambda 1549$), CIII ($\lambda 1909$), MgII ($\lambda 2798$), OIII ($\lambda 4363$, $\lambda 4959$, $\lambda 5007$), and the Hydrogen Balmer series.
- 7) Some quasars show narrow absorption lines often with several sets of red shifts usually less than the emission line of red shift.

12.4 RADIO PROPERTIES

The extragalactic sources can be conveniently divided into two groups; the extended or transparent sources, and the compact or opaque sources. The observed properties of the two groups are compared in Table I and are discussed

in more detail in the following pages.

Quite surprisingly there is no simple relation between the dimensions of the radio emitting region and the dimensions of the optical galaxy or QSO, and it must be emphasized that the division into compact and expanded radio sources in no way separates the quasars from the radio galaxies. In fact, insofar as we know for any individual source, the quasars are indistinguishable from the radio galaxies on the basis of their radio properties alone. There are, however, clear statistical differences; the majority of the compact sources are identified with quasars or with galaxies that have bright nuclei, such as N type or Seyfert galaxies. However, many also appear in normal looking elliptical galaxies as well. Likewise the extended radio sources are not identified only with galaxies, but are frequently associated with quasars showing no visible optical extent.

Because the compact sources are all affected by self absorption (see section 12.5.4), their spectra are flat and they are therefore most easily detected by radio surveys made at short wavelengths.

12.4.1 Brightness Distribution - The three dimensional structure of extragalactic sources is usually inferred from the observations of the angular size and brightness distribution projected onto the plane of the sky. Often only the brightness distribution in one dimension is determined. The data on brightness distributions are obtained by one of four common procedures.

a) Pencil Beam Observations: Only a few of the extragalactic sources are sufficiently large that their structure can be studied by even the largest pencil beam radio telescopes. Moreover, these sources are all relatively nearby of low absolute luminosity and very low surface brightness and do not therefore represent the typical extragalactic source.

b) Lunar Occultations: For a number of years the highest resolutions were obtained by means of observing the diffraction pattern of a radio source as it was occultated by the moon. Most of the analysis was based on a technique described by Scheuer (1962) and later extended by von Hoerner (1964) to restore the true brightness distribution from the observed Fresnel diffraction pattern. The maximum resolution is generally limited by the sensitivity of the telescope.

Although a radio telescope especially designed for this purpose has recently been completed in India, the technique has not enjoyed widespread use for several reasons:

1) High resolution is obtained only for very strong sources or when using very large antennas such as the 1000' Arecibo spherical reflector. The total integration is limited to less than one minute by the duration of the occultation, and very short receiver time constants are required to obtain maximum resolution.

2) Each occultation gives only a one dimensional "strip" distribution. Several occultations are required to reconstruct the two dimensional structure.

3) At the shorter wavelengths, the moon is an intense source of thermal radio emission and the small tracking irregularities present in radio telescopes may completely mask the occultation of the much weaker extragalactic sources.

4) Interference from terrestrial radio emission reflected from the moon is often a serious problem.

c) Interplanetary Scintillations: In 1962 a group working at the Cavendish Laboratory in England discovered that radio sources with structure of the order of a second of arc or less showed rapid scintillations when they passed near the solar corona. This effect was initially noticed by Doublas (1964) in studying the intense decameter bursts from the planet Jupiter.

For several years interplanetary scintillations (IPS) were used to investigate the small scale structure of radio sources. But more recently this work is being done by high resolution interferometers, and the IPS are used to study scintillations as a function of solar elongation.

d) Interferometry and Aperture Synthesis: During recent years the techniques of interferometry and aperture synthesis have been greatly expanded and are now providing accurate and detailed information on the structure of extragalactic sources. Because of the importance of these techniques, a whole chapter of this book has been devoted to describing the methods in considerable detail. The reader who is interested in further details about the application of lunar occultations and interplanetary scintillations is referred to the review by Cohen (1970).

The majority of the sources which have been studied have angular dimensions less than a few minutes of arc, and about half of all sources are less than 15" arc. For the resolved sources, a simple single component structure is very rare, and most sources show a surprising amount of structure. Often the source lies along a single axis and the most common configuration is the double structure where most of the emission comes from two well separated components. Frequently the two components have approximately equal size and luminosity. Typically, the overall dimensions are about three times the size of the individual components which are symmetrically located about the galaxy or QSO. But in some cases the ratio of component to separation to component size may be very great. Often an extended low surface brightness component is located between the two primary components.

Other sources show more complex structures which contain three or more distant components also usually aligned along a single axis (MacDonald et al. 1968; Fomalont, 1969). In all of these extended sources the radio emission comes primarily from regions well removed from the optical galaxy or quasar. High resolution studies of these extended clouds often show considerable structure with one or more highly condensed regions existing many kiloparsecs from what is presumed to be the parent galaxy or quasi stellar object. Typical linear dimensions for these extended sources range from about 10 kiloparsecs to several hundred kiloparsecs.

In some objects, such as quasars or Seyfert and N galaxies, but including some normal looking elliptical galaxies as well, there is one or more very compact radio source coincident with the region of brightest optical luminosity. These compact sources also have complex structure with component sizes ranging from about $0''.1$ arc second to well under $0''.001$. Often compact and extended components exist simultaneously. The extended components may appear as a) a "halo" surrounding a compact "core" component, as in the galaxy M87, b) a jet extending away from the compact component as in 3C273, or c) a pair of unconnected extended components laying on either side of the compact central source, as in 3C111. Generally the sources in category a) are identified with E galaxies and those in b) with N or Seyfert galaxies, or quasars.

The observations of the compact sources are made with independent oscillator-tape-recording interferometers (see Chapter 10) using widely spaced telescopes around the world with baselines up to 80% of the earth's diameter. Because intermediate baselines are insufficiently sampled, the data is not adequate to completely reconstruct the brightness distribution and resort must be made to model fitting. To the extent that the brightness distribution can be inferred

from the limited data, the structure of the compact sources appears remarkably similar to that of the extended sources, in the sense that in general, they do not show circular symmetry, but consist of two or more well separated components, lying along a single axis. Thus over a range of angular (and linear) dimension of about a factor of 10^5 , The radio sources show essentially similar structure, only the scale size varies.

The smallest linear size which has been directly measured is the compact source located in the nucleus of the nearby galaxies M87, which contains about 1% of the total flux density and is only about 0.1 parsec across in extent.

One of the best studied sources is the intense radio galaxy Cygnus A, which contains two components separated by about 2 min arc, with a galaxy halfway between. Each of the components is about 30 sec arc in size, and is somewhat elongated along the line joining the components. Near the outer edge of each of these components is an intense bright core. High resolution observations of the western core show that itself is a double source with a separation of about 5 arc sec along a position angle about 20° from the line joining the two main components. The eastern component is also a double with a separation of a few arc seconds along a line nearly perpendicular to the line joining the main components. Each of the subcomponents has an angular size of the order of one arc second. The small diameter components have a somewhat flatter spectrum than the surrounding regions (Miley and Wade 1971).

12.4.2 Polarization - Nearly all of the radio galaxies and quasars show some degree of linear polarization ranging from integrated values of a few tenths of a percent to several percent with the greatest value about 20%. At least for the extended sources, the integrated polarization is generally greatest at the shorter wavelengths, and the greatest polarizations are found

are found in the low surface brightness objects. In general the plane of polarization rotates at a rate approximately proportioned to λ^2 and it is generally considered that this is due to Faraday rotation. Since the amplitude and sign of rotation appears to depend on galactic coordinates, it is thought that most, but not necessarily all, of the rotation occurs within our own galaxy. The degree of depolarization at longer wavelengths may also depend on galactic coordinates but this is not clearly established.

Observations have also been made to map the distribution of polarized emission. In some cases the observed polarization reaches a degree of polarization comparable to that expected from a uniform magnetic field, and indicates remarkably aligned magnetic fields over large volumes of space. Generally the regions of lowest surface brightness show the greatest polarization. In the elongated sources the direction of the polarization is often along the line joining the components.

More recently, several workers have detected small amounts of circular polarization in a few compact sources.

12.4.3 Spectra - With the exception of the 21 cm line of neutral hydrogen found only in relatively nearby galaxies, there are no sharp features in the radio spectra of galaxies and quasars, and the observations are confined to measurements of the continuous spectra. Since, unlike optical telescopes, radio telescopes generally operate only over a limited range of wavelengths, the determination of spectra over a wide range of wavelengths requires combining data obtained by many observers using widely different types of

telescopes. Because radio telescopes may differ widely in their characteristics, each antenna and radiometer system must be separately calibrated at every wavelength where observations are made. Generally, this is done by observing one or more sources whose intensity had previously been determined on an "absolute" scale. Until recently, the problem of obtaining an "absolute" calibration of these primary standards was a formidable one and the experimental discrepancies discouragingly large. Today, however, the situation is vastly improved and standard sources calibrated with an absolute accuracy of 3%-10% are available over a wide range of wavelength. The determination of relative intensities is much easier and is routinely done to an accuracy of a few percent, at least at the shorter wavelengths where confusion from the galactic background is less important.

Hundreds of extragalactic sources have now been observed over a range of wavelengths extending from a few centimeters to a few meters, and a smaller number over the wider range from a few millimeters to a few tens of meters (10 MHz - 100 GHz). This range of 10^4 to 1 in wavelength may be compared with the range of only about 2:1 available for ordinary optical spectra. Although a wide variety of spectral shapes are found, no clear distinction exists between the spectra of radio galaxies and those of quasars. //

Radio spectra are usually displayed in the form of a logarithmic plot of flux density ^{v_s} frequency. Sources with simple power law spectra are then represented by a straight line. The spectral index, α , is defined by the relation (flux density) \propto (frequency) $^\alpha$. Since for most of the earlier known sources, the flux density decreased with wavelength, the spectral index was sometimes defined by (flux density) \propto (frequency) $^{-\alpha}$ so that α was always a positive number. Now that indices of both signs are known to occur, the definition given in text is being more widely used. $S \propto \nu^\alpha$

Although only a few sources accurately follow a simple power law, a spectral index may be defined at any frequency as the tangent to the curve on a $\log S - \log f$ plot, or by the measurement of flux density at two arbitrarily selected frequencies. The observed spectra are conveniently divided into three groups:

i) Sources where the flux density decreases monotonically over the entire range of observed frequencies - Class S (smooth). This is the form of spectra observed for the extended radio sources, which are optically thin at all wavelengths and can usually be represented by a single or dual power law with indices typically in the range -0.7 to -1.2 . In the case of the dual power law spectra, the slope is steeper at short wavelengths, and, the curvature in the spectrum extends over a decade or so of wavelength. At significantly longer or shorter wavelengths the sources usually have a well defined index, and the difference in the indices is $\gtrsim 0.5$. There are no class S spectra with indices flatter than -0.5 .

ii) Sources where the flux density decreases with frequency at high frequencies, but has a sharp cutoff at low frequencies which is probably due to self absorption (see 12.5.4) at wavelengths where the source becomes opaque to its own radiation - Class C (curved).

iii) Sources which have complex spectra showing one or more relative minima (CMX). These are thought to be composed of two or more Class C components which become opaque at different frequencies plus in some cases a (Class S) component.

The histogram of the distribution of spectral indices shows two distinct

populations. One, which predominates the surveys made at relatively long wavelengths, contain relatively steep type S spectra, with a narrow distribution of indices about a median value near -0.8 and a dispersion of 0.15 . The steepest value of the index which is observed is about -2.0 . Very few sources, however, have indices steeper than -1.3 . Although only one source, 3C318.1 has an index as steep as -2 over the whole observed frequency spectrum, several others, which have "normal" spectra at meter and decimeter wavelengths, have a "steep" ($\alpha \sim -2$) spectral component at dekameter wavelengths. The Class S spectra are associated with the extended radio sources discussed earlier.

The second population are found mostly in surveys made at shorter wavelengths, have flat spectra, and a much broader dispersion in spectral index about a median value roughly near zero. These are all C or CMX associated with compact sources. The preponderance of indices near zero, appears to be due to the fact that the form of the spectra in these sources are due to the superposition of a number of Class C components with spectral peaks extending over a range of frequencies.

For most of the extended radio sources where the radio brightness distribution has been mapped at several wavelengths, the structure is found to be essentially independent of wavelength. In other words, the spectral index is constant throughout the source. An exception to this, however, is the so-called "Core-Halo" source, in which the compact "core" component generally has a very flat spectrum due to synchrotron self absorption.

Although it is not possible in any individual case to distinguish between radio galaxies and quasars on the basis of their spectra, there does appear

to be statistical differences in the spectral distributions for the two classes of identifications. The radio galaxies show mostly of class S spectra, and as shown in figure _ have a narrow dispersion of indices near -0.8 . The small "tail" in the distribution toward flat spectra represent sources which are mostly identified with galaxies having prominent optical nuclei such as Seyfert or N galaxies, but several otherwise normal looking E galaxies are also included. In the case of the quasars, both spectral populations are represented, but the "flat spectra" population is considerably more prominent in the case of the galaxies.

See
figure

The unidentified sources selected from long wavelength surveys show a spectral distribution which is similar to that of the radio galaxies, although the mean index is somewhat steeper. It is thus possible to interpret these unidentified sources as radio galaxies which are beyond the plate limit of the Palomar Sky Survey. The slightly steeper mean index observed for these sources may be explained, if they have dual power law spectra, and the large red shift has moved the high frequency (steeper) part of the spectrum into the observed frequency range. Detailed investigation of the form of radio source spectra, however, indicate that the spectra do not steepen sufficiently at high frequencies to be interpreted in this way.

An alternate explanation is that if the identified sources are associated with radio galaxies beyond the plate limit, they must be relatively distant, and thus have a high absolute radio luminosity. The steep spectra observed for the unidentified sources then reflects the relation between high luminosity and steep spectra.

Because the sources with flat or inverted spectra are relatively weak at long wave wavelengths, they were not detected in the earlier surveys which were made

at meter wavelengths. As techniques have been pushed toward shorter wavelengths, the fraction of flat spectra sources detected by surveys has increased. Near 6 cm wavelength the observed fraction of flat spectra (opaque) sources and steep spectra (transparent) sources is about equal. The expected dependence of the spectral index on observing wavelength may be easily calculated, given the normalized spectral index distribution, $P(\alpha)$ at any wavelength ν_1 for sources with flux density stronger than S_1 , provided that $P(\alpha)$ is independent of S , the spectral distribution, $Q(\alpha)$ for all sources stronger than S_2 at ν_2 .

$$Q(\alpha) = \frac{N[(\nu_2/\nu_1)^{-\alpha} S_2, \nu_1]}{N(S_2, \nu_2)} P(\alpha) \quad (12.1)$$

where $N(S, \nu)$ is the integral number flux density relation (see Chapter 13).

If $N(S) \propto KS^x$ where K and x are constants, then

$$Q(\alpha) = \frac{N(S_2, \nu_1)}{N(S_2, \nu_2)} \left(\frac{\nu_2}{\nu_1} \right)^{-\alpha x} P(\alpha) \quad (12.2)$$

where the first term is simply a normalization constant.

In the special case where $P(\alpha)$ is a gaussian with mean index α_0 and dispersion σ , then $Q(\alpha)$ is also Gaussian with the same dispersing σ but with a mean index displaced by the amount

$$\Delta\alpha = x\sigma^2 \ln \nu_1/\nu_2 \quad (12.3)$$

Because of the factor $\left(\frac{\nu_2}{\nu_1}\right)^{-\alpha x}$ in equation 12.2, it is clear that spectral index distribution is very frequency dependent and that sources with flat spectra dominate short wavelength surveys in the same way that steep spectra dominate the long wavelength surveys. For example, if the slope, x , of the $\log N - \log S$

relation is taken as 1.5 then the ratio of flat spectra ($\alpha > 0$) to steep spectra ($\alpha = -1$) sources over a 10 to 1 frequency interval is $10^{1.5} = 32$.

This change in the spectral index distribution with sample frequency should not be confused with the observed change in the index distribution when a given sample of sources is observed at different wavelengths. By contrast, the brightest n sources which determine $P(\alpha)$ at ν_1 are not the same n sources which determine $Q(\alpha)$ at ν_2 .

Comparisons of surveys made at different wavelengths, and of the dependence of the spectral index distribution on wavelength are in reasonable agreement with that predicted by the expressions above. This means that the full range of spectral population is represented at each observing frequency, although the relative fraction may vary considerably.

12.4.4 Intensity Variations - Many of the compact sources show pronounced intensity variations on time scales from less than a week to a few years. There is no simple pattern to the observed variations; in particular, there is no evidence for any periodic phenomena. Rather the variations appear as bursts, first at short wavelengths, and then at longer wavelengths with reduced amplitudes with the duration of each burst being longer at the longer wavelengths. Below some critical wavelength, the amplitude and shape of the bursts, and its time of occurrence is independent of wavelength. Often the duration of a single outburst is comparable to the time between outbursts so that the individual events are not resolved.

Quasars and the nuclei of some galaxies may also vary at optical wavelengths. Although there appears to be no detailed relation between the intensity variations seen at radio and optical wavelengths, those sources which are most active at radio frequencies, are also usually prominent optical variables.

There is no obvious difference in the pattern of the radio intensity variations seen in radio galaxies and quasars. The change in radiated power

observed in the radio galaxies is typically of the order of 10^{42} ergs/sec/year. For the quasars, if they are cosmological distances, the change is very much greater and may be as much as 10^{45} ergs/sec/year or comparable with the total radio luminosity of the strongest radio galaxies such as Cygnus A.

Variations are also observed in the polarization of the compact extragalactic sources. These measurements are very difficult since the observed polarization is typically only a few percent, and so the experimental uncertainties are large. The limited data indicate that the most rapid changes in polarization occur when the total flux is increasing or is near a maximum (e.g. Aller 1970).

12.4.5 Empirical Relations - The establishment of relations between the various observed radio source properties is clearly important to the understanding of the origin and evolution of extragalactic sources. Some of the better determined relations are summarized below. Some of these are well understood in terms of current theory. Others are not.

1) Spectral index - angular size. All of the sources with flat or inverted spectra ($\alpha \geq -0.5$) have small angular dimensions ($\theta \ll 1''$). This is well understood as the effect of self absorption.

2) Spectral-index variability. All of the sources which show flux density variations have flat and CPX spectra ($\alpha \geq -0.5$) in the spectral region where the intensity varies. This is a reflection of the fact that only the opaque or partially opaque sources vary. Sources which have a single sharp low frequency cutoff generally do not vary.

3) Radio-optical variability. Sources which show large radio flux density variations also frequently show large variations at optical wavelengths as well, but there is no simple one to one relation.

4) Variability-wavelength. The largest and most rapid variations generally occur at the shorter wavelengths.

5) Spectral Index-Luminosity. Among the extended transparent radio galaxies there is a tendency for the most luminous sources to have the steepest spectra (Heeschen 1966). This relation does not seem to hold, however, for the quasars which all have a very high radio luminosity.

6) Luminosity-Structure. Sources with relatively simple brightness distributions are of relatively low luminosity.

7) Luminosity-Brightness. Sources with a high surface brightness have a high radio luminosity. Two sequences are apparent as shown in figure .

8) Polarization-wavelength. For the transparent sources (Class S spectra) the observed polarization is greatest at shorter wavelengths. In the opaque sources the reverse is true.

9) Circular polarization is found only in opaque sources.

10) The greatest linear polarization is found in the sources with low surface brightness, or in low surface brightness regions of resolved sources.

11) Sources found in clusters tend to have smaller dimensions.

12) The strong radio galaxies nearly all show intense emission lines.

13) The two most rapidly varying sources, BL Lac and OJ287, appear to be quasars, but their optical spectra do not show the emission lines common to other quasars.

12.5 THEORIES OF RADIO SOURCES

Theories describing the source of energy in radio galaxies and quasars have been as numerous and varied as the authors proposing them. These theories which, in general, make no attempt to interpret the growing detailed observational

data including

- a) the collisions of stars or galaxies;
- b) the collapse of stars, superstars, or galaxies
- c) the explosion of stars, superstars, or galaxies, including chain reactions;
- d) Matter - anti matter annihilation;
- e) interactions.

In recent years, however, there has been a noticeable de-emphasis in producing exotic energy sources, and theoretical efforts have concentrated on interpreting the observed spectra, polarization, structure, and time variations in terms of the synchrotron hypothesis.

For many years nearly all of the theoretical effort in this direction was occurred in the Soviet Union (e.g. Shklovsky and Ginzburg 19). Today, however, the synchrotron model is widely accepted, and it may be hoped that an increased understanding of the observational material in terms of synchrotron radiation will lead to a better understanding of the source of energy. In particular, the exciting discovery by Dent in 1965 of rapid time variations in the radio emission of some quasars and galaxies has opened the possibility of observing the synchrotron emission from relativistic particles within a few months to a few years of the time they are accelerated. This offers a previously unexpected opportunity to study the source at a very early epoch and may ultimately specify the initial conditions in radio sources, and thus uniquely specify the source of energy.

In the remainder of this section we summarize briefly the basic results of the synchrotron theory as they apply to radio astronomy and then the theory is applied to the data in an attempt to understand the origin and evolution of

extragalactic radio sources. A thorough review of the basic synchrotron process is given in the book by Pacholizyk (1970).

12.5.1 Synchrotron Radiation - A single electron spiraling in a magnetic field at ultra relativistic velocities $[(1 - v^2/c^2) \ll 1]$ has its radiation concentrated in a cone of half angle $\theta \sim E/mc^2$. An observer sees a short burst of emission lasting only during the time, Δt , that the cone is pointed toward the observer. $\Delta t \sim 1/w \sim (mc^2/E)^2$. The radiation is concentrated in the high order harmonics, $n = (E/mc^2)^2$, of the classical gyro frequency $\nu_g = eB/m$. The frequency distribution of the radiation is given by a complex expression conveniently represented by (eqn. 1.7).

$$P(\nu, E, \theta) = 2.3 \times 10^{-29} B_{\perp} \nu/\nu_c F(\nu/\nu_c) \text{ watts Hz}^{-1} \quad (12.4)$$

where

$$F(\nu/\nu_c) = \int_{\nu/\nu_c}^{\infty} K_{5/3}(n) dn \quad (12.5)$$

and where $B_{\perp} = B \sin \theta$ is the component of the magnetic field perpendicular to the line of sight; $K_{5/3}(n)$ is a modified Bessel function; θ is the angle between the electron trajectory and the magnetic field (pitch angle); and the critical frequency ν_c is given by

$$\nu_c = c B_{\perp} E_{\text{Gev}}^2 \text{ MHz} \quad (12.6)$$

The spectrum of the observed radiation depends on the angle ϕ between the line of sight and the electron trajectory and on the plane of polarization. In the remainder of this chapter the subscript is dropped and the symbol B is understood to represent the perpendicular component of the magnetic field.

The total power radiated by each electron is given by

$$dE/dt = A B_1^2 E_{\text{GeV}}^2 \text{ ergs/sec.} \quad (12.7)$$

where $A = 6.08 \times 10^{-9}$ and $c = 1.6 \times 10^7$.

The distribution given by equation (12.4) has a broad peak near $\nu \sim 0.28 \nu_c$. For $\nu/\nu_c < 0.3$, $P(\nu) \propto \nu^{1/3}$, and for $\nu/\nu_c > 3$, $P(\nu) \propto (\nu/\nu_c)^{1/2} e^{-\nu/\nu_c}$ and the radiation rapidly falls off with increasing frequency.

For an assembly of electrons with a number density $N(E)dE$ between E_1 and E_2 , equation (12.4) can be integrated to find the total radiation at any frequency from all electrons. Using (12.6) and making a change of variable this becomes

$$P(\nu_1, \theta) = 4.1 \times 10^{-29} B^2 \nu^{1/2} \int_{\nu/\nu_1}^{\nu/\nu_2} (\nu/\nu_c)^{-3/2} N(\nu/\nu_c) F(\nu/\nu_c) d(\nu/\nu_c) \quad (12.7)$$

where ν_1 and ν_2 are the critical frequencies defined by eqn (12.6) corresponding to E_1 and E_2 .

In the special case where the electron energy distribution is a power law, that is, $N(E) dE = K E^{-\gamma} dE$, equation (12.7) becomes (eqn. 1.9).

$$P(\nu_1, \theta) \propto B^{(\gamma+1)/2} \nu^{-(\gamma-1)/2} \int_{\nu/\nu_1}^{\nu/\nu_2} (\nu/\nu_c)^{-(3-\gamma)/2} F(\nu/\nu_c) d(\nu/\nu_c) \quad (12.8)$$

for $\gamma \gtrsim 1$ the major contribution to the integral is when $\nu/\nu_c \sim 1$ so that the limits of integration may be extended from zero to infinity with introducing significant error. The integral is then essentially constant when $3\nu_1 \lesssim \nu \lesssim 10\nu_2$. The radio spectrum then is a power law with a spectral index $\alpha = -(\gamma - 1) / 2$.

(12.9)

It must be emphasized that this approximation is only valid when $\gamma \gg 1$; and in particular that no form of energy distribution can give a spectrum that rises faster than the low frequency asymptotic limit of $\nu^{1/3}$ for a single electron.

As described in section 12.4.3, many sources show nearly power law radio frequency spectra with a common spectral index $\alpha \sim -0.8$ corresponding to an electron energy distribution index, $\gamma \sim 2.6$. Deviations from a constant radio spectral index may be explained as being due to (a) variations in γ as a function of energy which may exist either in the initial electron energy distribution or occur as a result of differential energy loss in an initially straight distribution; (b) self absorption in the relativistic electron gas; (c) absorption in a cold H II region between us and the source; (d) the effect of a dispersive medium in which the electrons are radiating.

12.5.2 Effect of Energy Losses - Even if relativistic electrons are initially produced with a power law distribution differential energy losses can alter the energy spectrum. Relativistic electrons lose energy by synchrotron radiation and by the Inverse Compton effect which are both proportional to the square of the energy; by ordinary bremsstrahlung and adiabatic expansion which are directly proportional to the energy, and by ionization which is approximately proportional to the logarithm of the energy. Approximating the logarithmic term by a constant the rate of energy loss may be written

$$\frac{dE}{dt} = aE^2 + bE + c \quad (12.10)$$

If electrons are being supplied to the source at a rate $Q(E, t)$, then the equation of continuity describing the time dependence of the energy distribution $N(E, t)$ is

$$\frac{\partial N(E, t)}{\partial t} = -\frac{\partial}{\partial E} \left(\frac{dE}{dt} N(E, t) \right) + Q(E, t) \quad (12.11)$$

If at $t = 0$

$$N(E) = \begin{cases} K E^{-\gamma} & E_1 < E < E_2 \\ 0 & E < E_1, E > E_2 \end{cases} \quad (12.12)$$

and if synchrotron and Inverse Compton losses dominate and there is no injection of new particles ($Q(E,t) = 0$), then

$$N(E, t) = \begin{cases} \frac{K E^{-\gamma}}{(1 - AB^2 Et)^{2-\gamma}} & E_1' < E < E_2' \\ 0 & E < E_1', E > E_2' \end{cases} \quad (12.13)$$

where

$$E' = E / (1 + AB^2 Et)$$

Thus, even with an initial energy distribution extending to unlimited energy, there will be a cutoff at

$$E_c = 1 / AB^2 t \quad (12.14)$$

and a corresponding cutoff in the synchrotron radiation spectrum. In the special case where $\gamma \sim 2$, $N(E,t)$ can become very large for energies slightly less than E_c because of the piling up near E_c of electrons with large initial energies as the result of their more rapid rate of energy loss. In this case, if E_2 is sufficiently large so that $E_2'/E_c \sim 1$, then the radiation spectrum will become flat just below the upper cutoff frequency, $\nu_c = c BE_c^2$. Above ν_c , the spectrum sharply decreases rapidly for all values of γ .

If the distribution of electron pitch angles is random, then the cutoff frequency for each pitch angle differs and at low frequencies where energy losses are not important the spectral index, α , remains equal to its initial value $\alpha_0 = (1 - \gamma)/2$. But at higher frequencies if the pitch angle distribution is consumed (Kordashev 1962), $\alpha = (4/3 \alpha_0 - 1)$. If on the other hand, the pitch angles get mixed up, then all the electrons see the same effective magnetic field and the spectrum shows the same sharp cutoff observed with a single pitch angle. The frequency separating the two spectral regions is given by

$$\nu_b \sim B^{-3} t^{-2} \text{ years} \text{ GHz} \quad (12.15)$$

If the relativistic electrons are continuously injected with $Q(E) = K E^{-\gamma}$, then for $\nu < \nu_b$ the spectral index remains constant with $\alpha = \alpha_0$. But at higher frequencies where the rate of energy loss is balanced by the injection of new particles the equilibrium solution of equation (12.11) with $\frac{\partial N}{\partial t} = 0$, gives $\alpha = (\alpha_0 - 1/2)$.

12.5.3 Interpretation of Spectral Data - The main features of the radio spectra which must be explained by any theory of the generation of the relativistic particles are

- a) the relatively sharp concentration of the energy index, $\gamma \sim 2.6$;
- b) the extreme values of the index for the class S spectra of $\alpha \sim -0.5$ and $\alpha \sim -2.0$, and the inclusion of nearly all sources in the range $-0.5 > \alpha > -1.3$;
- c) the absence of any sharp high frequency cutoff in the radio spectra expected from synchrotron radiation losses;
- d) the detailed form of the spectra of the transparent sources;
- e) the observed index $\alpha \sim -0.25$ for the transparent part of the spectrum of the variable sources.

The last point suggests that the initial value of the spectral index $\alpha_0 \sim -0.25$ ($\gamma \sim 2$). The high probability of finding an observed index steeper than α_0 by about 0.5 suggests the continuous ejection model, and the limiting value of -1.3 suggests instantaneous ejection with $\alpha = 4/3(-.25) - 1 = -1.33$. Both of these can be accounted for by assuming that there is a receiving generation of particles with a characteristic period T. Then from equation 12.15 the spectral index after an elapsed time $t \gg T$

$$\begin{array}{ll} \text{i} & \alpha = \alpha_0 \quad \nu < B^{-3} t^{-2} \\ \text{ii} & \alpha = \alpha_0 - 1/2 \quad B^{-3} t^{-2} < \nu < B^{-3} T^{-2} \\ \text{iii} & \alpha = 4/3 \alpha_0 - 1 \quad \nu > B^{-3} T^{-2} \end{array}$$

In case i, the effect of synchrotron radiation losses are not important, and the index remains equal to its initial value. In case ii the time scale for radiation loss is longer than the period T between bursts, the injection can be considered quasi-continuous, and the spectrum is in equilibrium since radiation losses are balanced by the injection of new particles. In case iii, synchrotron losses dominate and the spectrum steepens. The observed curvature in the spectrum of many sources is also consistent with this model.

The problem with the recurring injection model is that the high frequency part of the spectrum, $\alpha = (4/3 \alpha_0 - 1)$, can be understood only in the unlikely case where the electron pitch angles are conserved for times greater than the radiation lifetime, which for $B = 10^{-4}$ and $\nu = 1$ GHz is 10^6 years. Otherwise, the spectrum must show a sharp cutoff at high frequencies unless in fact the relativistic electrons lose energy not by synchrotron radiation but by some other means.

12.5.4 Effect of Absorption by Ionized Hydrogen - The observed radio spectrum may differ from the radiated spectrum due to the influence of the medium between the source and observer. If a cold cloud of ionized gas is located in front of the source, then the observed flux density will fall off sharply below the frequency, ν_0 , where the optical depth is unity. For an electron temperature T_e

$$\nu_0 \sim 3.6 \times 10^5 T_e^{-3/2} \epsilon \text{ MHz} \quad (12.16)$$

where $\epsilon = \int n_e d\ell$ is the emission measure, and n_e the density of thermal electrons. The observed spectrum is then

$$S \propto f^\alpha e^{-(\nu_0/\nu)^2} \quad (12.17)$$

If the ionized medium is mixed with the synchrotron source, then for $\nu \ll \nu_0$

$$S \propto \nu^{(\alpha + 2)} \quad (12.18)$$

If the density of thermal electrons is sufficiently great then at frequencies where the index of refraction, n , becomes less than unity, the form of the spectrum will differ from that in vacua. When $n < 1$, the velocity of a relativistic electron is less than the phase velocity of light in the medium; the radiation is no longer so highly concentrated along the electron trajectory, and the energy no longer appears in the high order harmonics of the gyro frequency. This is commonly called the Razin or Tsytovich effect and is important when

$$\nu_r \lesssim 20 \frac{n_e}{B} \text{ MHz.} \quad (12.19)$$

For $\nu < \nu_r$ the spectrum cuts off very sharply (see Chapter 3.3).

12.5.5 Synchrotron Self Absorption - In sections 5.2 and 5.3 we have assumed that the flux from a group of relativistic electrons is merely the arithmetical sum of the radiation of each electron, i.e., the electron gas is assumed to be transparent. If, however, the apparent brightness temperature of the source approaches the equivalent kinetic temperature of the electrons, then self absorption will become important and part of the radiation is absorbed. The precise form of the radiation spectrum is complex, but can be calculated from the emission and absorption coefficients of relativistic electrons in a magnetic field. The parameters depend on the electron energy and pitch angle distributions and can be determined only from numerical integrations. The form of the spectrum in the limiting case of a completely opaque source may be derived quite straightforwardly, however. Consider the radiation from an optically thick black body of solid angle Ω at temperature T . Then the observed flux density is then

$$S = \frac{2k}{c} \nu^2 T \Omega \quad (12.20)$$

If the optically thick relativistic electron gas is described as a black body whose temperature is given by the equivalent kinetic temperature of the electrons, $E = kT$, then using (12.16) we can write

$$S \sim 10^{-3} B^{-1/2} \theta_{\text{sec}}^2 \nu^{2.5} \text{ f.u.} \quad (12.21)$$

In other words, the source may be thought of as a black body ($S \propto \nu^2$) whose temperature (energy) depends on the square root of the frequency ($E \propto \nu^{1/2}$).

Rewriting equation (12.21) and using a more precise analysis including the small dependence on the index, γ , and the effect of the red shift, z , the

magnetic field is given by

$$B \sim g(\gamma) (S_m / \nu_m^2)^{-2} \nu_m^5 (1+z)^{-1} \quad (12.22)$$

where $g(1.5) = 2 \times 10^{-6}$ and $g(2.5) = 2.6 \times 10^{-6}$, and where S_m is the maximum flux density at the self absorption cutoff frequency, ν .

Although the apparent effect of synchrotron self absorption is evident in many sources where indices as steep as $\alpha \sim +1$ are often observed at long wavelengths, there has not been any direct observation of the theoretically expected value of +2.5. This has led some to question whether or not the observed low frequency cutoffs are in fact due to self absorption. However, this argument is probably irrelevant for the same reason that the theoretical index of $\alpha = +2.0$ is never observed in the thermal emission spectra of the familiar H II regions. The explanation in both cases is that there is a wide range of opacities in these sources which cause different parts of the source to become opaque at different wavelengths producing a gradual, rather than sharp, transition from the transparent to opaque case.

12.5.6 Inverse Compton Scattering - The maximum brightness temperature of any opaque synchrotron source is limited by inverse Compton scattering to about 10^{12} °K. This is the brightness temperature corresponding to the case where the energy loss by synchrotron radiation is equal to the energy loss by inverse Compton scattering and may be derived as follows (Kellermann and Pauliny-Toth 1969).

For an homogeneous isotropic source

$$\frac{L_c}{L_s} = \frac{U_{\text{rad}}}{U_H} = 6 \frac{L}{\rho^2} B^2 c = \text{const} (S_m \nu_c R^2) / R^2 \theta^2 B^2 c \quad (12.23)$$

where L_c = power radiated by inverse Compton scattering, L_s = radio power radiated by synchrotron emission, $4\pi r^2 \int_0^{\nu_c} S \, d\nu \sim S_m \nu_c$, $U_{\text{rad}} = 3L/4\pi r^2 c =$ energy density of the radiation field, $U_B = B^2/8\pi$ energy density of the magnetic field, D = the distance to the source, θ the angular size, and $\rho = D\theta/2$ the radius. Then using equation (12.22) and recognizing that $S_m/\theta^2 \nu^2$ is proportional to the peak brightness temperature, T_m , and including the effect of second order scattering, we have

$$\frac{L_e}{L_s} \sim \frac{1}{2} (T_m/10^{12})^5 \nu_c \left[1 + \frac{1}{2} (T_m/10^{12})^5 \nu_c \right] \quad (12.24)$$

where ν_c is the upper cutoff frequency in MHz. Taking $\nu_c \sim 100$ GHz, then for $T_m < 10^{11}$ °K $L_c/L_s \ll 1$ and inverse Compton scattering is not important; but for $T_m > 10^{12}$ °K, the second order term becomes important $L_c/L_s \sim (T_m/10^{12})^{10}$ and the inverse Compton losses become catastrophic. The exact value of T_m corresponding to $L_c/L_s = 1$ is somewhat dependent on the specific geometry, the value of γ , and the spectral cutoff frequency ν_c , but the strong dependence of the ratio on T_m implies that T_m cannot significantly exceed 10^{12} °K, independent of wavelength.

If the compact sources expand with conservation of magnetic flux, then T_m varies with radius ρ as

$$T_m \propto \rho^{-(\gamma-1)/(\gamma+4)}, \quad (12.25)$$

so that for $\gamma \sim 1$, T_m remains constant and otherwise depends only weakly on ρ .

12.5.7 Energy Considerations - The problem of the origin and evolution of extragalactic radio sources has been of the major unsolved problems of theoretical astrophysics; in particular the source of energy needed to account for the large

power output and the manner in which this energy is converted to relativistic particles is still a mystery. Assuming only that synchrotron radiation from ultrarelativistic electrons is responsible for the observed radiation, the necessary energy requirements may be estimated in a straightforward way.

If the relativistic particles have a power law distribution with an index γ between E_1 and E_2 , then for $\gamma \neq 2$, the energy contained in relativistic electrons is

$$\epsilon_e = \int_{E_1}^{E_2} EN(E) dE = \frac{k}{2-\gamma} \left[E_2^{(2-\gamma)} - E_1^{(2-\gamma)} \right] \quad (12.26)$$

The constant K can be evaluated if the distance to the source is known; then the total luminosity of the source L may be estimated by integrating the observed spectrum, giving

$$L = \int_{E_1}^{E_2} N(E) \frac{dE}{dt} dE = \int_{E_1}^{E_2} AH^2 E^{(2-\gamma)} dE = A \frac{KB^2}{(3-\gamma)} \left[E_2^{(3-\gamma)} - E_1^{(3-\gamma)} \right] \quad (12.27)$$

and eliminating K

$$\epsilon_e = \frac{3-\gamma}{2-\gamma} \frac{E_2^{(2-\gamma)} + E_1^{(2-\gamma)}}{E_2^{(3-\gamma)} - E_1^{(3-\gamma)}} \frac{L}{A} \quad (12.29)$$

Using equation (12.6) to relate E_2 and E_1 to the cutoff frequency, and grouping all the constant terms together

$$\epsilon_e = C_e LB^{-3/2} \quad (12.30)$$

The magnetic energy is just

$$\epsilon_m = \int \frac{B^2}{8\pi} dV = C_m B^2 V \quad (12.31)$$

The total energy in fields and particles ($\epsilon_e + \epsilon_m$) is minimized when

$$\frac{\partial \epsilon}{\partial t} = 0 \quad (12.32)$$

or when

$$B = \frac{3}{4} \left(\frac{C_e}{C_m} \right)^{2/7} \frac{L}{V} \quad (12.33)$$

The constants C_e , C_m , and C_e/C_m are given in figure for several values of .

From equation (12.30), (12.31), and (12.33),

$$\epsilon_e = \frac{4}{3} \epsilon_m \quad (12.34)$$

That is, the energy is nearly equally distributed between relativistic particles and the magnetic field.

Typically, the total energy contained in the extended sources estimated in this way is in the range $10^{57} - 10^{61}$ ergs. and the magnetic field between 10^{-5} and 10^{-4} Gauss. It is largely because of this apparent very great energy requirement (up to 0.01% of the rest energy of an entire galaxy) that theoretical efforts to explain the origin of radio galaxies have been for the most part unsuccessful.

One interesting result is that if $\epsilon_e \sim \epsilon_m$ the total energy strongly depends on the size of the source ($\epsilon \propto r^{-9/7}$). This gives the curious situation that the larger sources with low surface brightness and low luminosity such as Centauria A contain, appear to contain more energy than the smaller high surface brightness objects such as Cygnus A. This is not, of course, what would be expected if, as generally assumed, the larger sources were older and has led to the interesting suggestion that sources may collapse rather than expand. Another way out of this situation which also reduces the energy requirements on the

larger sources is that if, as recent observations suggest, sources break up into a number of small components only a small fraction, ϕ of the projected volume of a source actually has particles and a magnetic field. The minimum total energy is then multiplied by a factor of $\phi^{3/7}$ and the corresponding magnetic field is increased by the factor $\phi^{-2/7}$.

For some years it was widely thought that the relativistic electrons were secondary particles produced as the result of collisions between high energy protons. If the ratio of energy in protons to that in electrons is, k , then the minimum total energy is increased by a factor of $(1+k)^{4/7}$ and the magnetic field by $(1+k)^{2/7}$. Estimates of the value of k were about 100 so the energy requirements are about an order of magnitude greater. However, the discovery of rapid time variations in many sources, and its implications for the rapid production of particles suggests that the secondary production mechanism is probably not relevant, and unnecessarily exaggerates the energy requirements. This elimination of the factor k , and inclusion of the factor ϕ , can easily reduce the energy estimates by two or more orders of magnitude.

A characteristic lifetime for radio sources may be estimated from the relation $t = \epsilon / (dE/dt)$. Lifetimes of radio sources determined in this way are very long. For $\epsilon \sim 10^{60}$ and $E/dt \sim 10^{45}$ ergs/sec the lifetime is 10^8 to 10^9 years. Similar ages are obtained from the fraction ($\sim 10\%$) of giant elliptical galaxies that are found to be strong radio sources, and an estimated age of 10^{10} years for the age of elliptical galaxies.

For the compact opaque sources magnetic field strength is given directly by the measured surface brightness, the frequency of maximum flux density and equation (12.22). For the relatively nearby radio galaxies with small red shifts the magnetic field derived in this way is independent of the red shift, and in any case depends only weakly on the red shift. If the distance is known, then the total energy in the form of relativistic particles, ϵ_p is given by the relation

$$\epsilon_p = P(\delta) \ell^2 \left(S_{\max} / \theta^2 \right)^{+3} v_m^{-(4\delta+11)/z}, \quad (12.35)$$

and the magnetic energy, ϵ_m , by

$$\epsilon_m = M(\delta) \ell^3 \left(S_{\max} / \theta^2 \right)^4 v_m^{10} \quad (12.36)$$

While the ratio of the two quantities is given by

$$R(\zeta) \approx \epsilon^{-1} \left(\frac{S_{\max}}{\theta^2} \right)^{\zeta+7} v_m^{-(4\zeta+31)/2} \quad (12.37)$$

Values of $P(\zeta)$, $M(\zeta)$, and $R(\zeta)$ are given in figure

Although the energies calculated in this way are very sensitive to the observed size and self absorption cutoff frequencies, good estimates of the energy content can be made at least for those sources where there is accurate data. For the relatively nearby compact radio galaxies, such as NGC 1275 the energy content is $\sim 10^{52}$ ergs. If the compact quasars are at cosmological distances, their energies are considerably greater and are about $10^{58 \pm 2}$ ergs. These values are both very much less than the minimum energy of the extended sources, so that it is clear that a single compact source does not simply evolve by expansion into an extended source.

12.5.6 Polarization - The synchrotron radiation from a single electron is elliptically polarized, and the degree of polarization is a function of v/v_c . In a uniform magnetic field the linear polarization of an ensemble of electrons with a power law index ζ , the polarization in the transparent part of the spectrum which is perpendicular to the magnetic field is

$$P(\zeta) = \frac{3\zeta+3}{3\zeta+7} \quad (12.38)$$

and is of the order of 0.7 for typical values of ζ . In the opaque part of the spectrum, the polarization is much lower and is given by

$$P(\zeta) = \frac{3}{6\zeta+13} \quad (12.39)$$

and is typically only about 10%.

Since the observed polarization in the transparent sources is typically only a few percent, it may be concluded that the magnetic fields are generally tangled, and so the observed polarization integrated over the source is greatly reduced. This is confirmed by the limited observations of polarizations approaching the theoretical value in limited regions of some sources, although it is somewhat remarkable that such highly ordered fields can exist over regions extending up to 10 or more kpc.

In the elongated sources the orientation of the polarization vectors indicate that the magnetic field is often aligned perpendicular to the direction of elongation. In some sources there appears to be a radial magnetic field.

If the pitch angle distribution is non isotropic, then there is a net circular polarization since the circularly polarized components of the individual electrons do not completely cancel. Even if the distribution is isotropic, there will be a small net circular polarization since there are more electrons in the solid angle defined by $\theta + d\theta$, than in the one $\theta - d\theta$. This effect is particularly important if the cone of radiation of a single electron $\theta \sim E/m^2$ is large as will occur at very low frequencies or in regions of high magnetic field strength.

12.5.8 Interpretation of Time Variations - The observations of time variations provides direct evidence in some sources of repeated energetic events which may provide a nearly continuous input of energy necessary to account for the observed energy requirements of the extended sources.

The form of the observed intensity variations are most simply interpreted in terms of a cloud of relativistic particles which is initially opaque out

to short wavelengths, but which, due to expansion, becomes optically thin at successively longer wavelengths. In its simplest form the model assumes that the relativistic particles initially have a power law spectrum, are produced in a very short time in a small volume of space, that the subsequent expansion occurs at a constant velocity, and that during the expansion the magnetic flux is conserved.

Thus

$$N(E,t,r) = K E^{-\gamma} \delta(\theta) \delta(t) \quad (12.40a)$$

$$\theta_2/\theta_1 = t_2/t_1 \quad (12.40b)$$

$$B_2/B_1 = (\theta_1/\theta_2)^2 = (t_1/t_2)^2 \quad (12.40c)$$

where θ is the angular dimensions, t the elapsed time since the outburst, B the magnetic field, and the subscripts 1 and 2 refer to measurements made at two epochs t_1 and t_2 . A detailed mathematical description of the model is given by van der Laan (1966) and is summarized below.

The observed flux density as a function of frequency, ν , and time, t , is then given by

$$S(\nu, t_2)/S_{m1} = (\nu/\nu_{m1})^{5/2} (t_2/t_1)^3 \left[1 - \exp(-\tau(\nu/\nu_{m1})^{-(\gamma+4)/2} (t_2/t_1)^{-(2\gamma+3)}) \right] \left[1 - \exp(-\tau) \right]^{-1} \quad (12.41)$$

If the optical depth is taken as the value of τ at the frequency, ν_m , which the flux density is a maximum, then it is given by the solution of

$$e^{\tau \nu} - \left(\frac{\gamma+4}{5} \right) \tau \nu - 1 = 0 \quad (12.42)$$

The maximum flux density at a given frequency as a function of time occurs at a different optical depth τ_t given by the solution of

$$e^{\tau_t} - \frac{2\gamma+3}{3} - 1 = 0 \quad (12.43)$$

Values of τ_v and τ_t as a function of γ are shown in figure .

In the region of the spectrum where the source is opaque, the flux density increases with time as

$$S_2/S_1 = \left(t_2/t_1\right)^3 \quad (12.44)$$

Where it is transparent it decreases as

$$\frac{S_2}{S_1} = \left(\frac{t_2}{t_1}\right)^{-2\gamma} \quad (12.45)$$

The wavelength λ_m at which the intensity is a maximum is given by

$$\frac{\lambda_{m2}}{\lambda_{m1}} = \left(\frac{t_2}{t_1}\right)^{(4\gamma + 6)/(\gamma + 4)} \quad (12.46)$$

and the maximum flux density S_m , at that wavelength is given by

$$\frac{S_{m2}}{S_{m1}} = \left(\frac{\lambda_{m2}}{\lambda_{m1}}\right)^{-(7\gamma + 3)/(4\gamma + 6)} \quad (12.47)$$

In most variable sources the outbursts occur so rapidly that the emission from different outbursts overlap both in frequency and time and so a detailed quantitative analysis is difficult. To the extent that it has been possible to

separate events in some sources, the individual outbursts seem to follow surprisingly well the simple model of a uniformly expanding cloud of relativistic particles. The data indicate that the initial value of γ is in the range 1 to 1.5 so that the initial radio spectrum in the optically thin region is very flat. At least for one year following an outburst the expansion appears to continue at a constant rate and the value of γ is unchanged by radiation losses or by inverse Compton scattering.

Initially the magnetic field strength may be as high as 1 gauss, and in those sources where there is good data the magnetic flux appears to be approximately conserved, at least during the initial phases of the expansion. But because the data from long-baseline interferometer observations when used in eqn. 12.22 indicate that $B \sim 10^{-4}$ Gauss over a wide range of dimensions for both variable and non variable sources, and since this is also the value of the field estimated from minimum energy arguments, it appears that the flux is conserved for only a limited time after which the relativistic particles diffuse through a fixed magnetic field of about 10^{-4} Gauss. In this way many repeated outbursts may provide the particles in the extended sources.

In the case of the variable radio galaxies, whose distance can be determined from their red shift, the initial dimensions appear to be well under one light year and the initial particle energy in a single outburst about 10^{52} ergs. Repeated explosions lasting up to 10^8 years at a rate of once per year are required to account for the minimum total energy in the extended sources.

The direct measurement of the angular size and expansion rate of variable sources using long baseline interferometry is now possible, and can be used to determine uniquely the magnetic field (eqn. 12.18), and when the distance is

known the total energy involved in each outburst (eqns. 12.25 and 12.27).

The model of a uniform, isotropic, homogeneous, instantaneously generated sphere of relativistic electrons, which expands with a uniform and constant velocity, where magnetic flux is conserved, and where the only energy loss is due to expansion is mathematically simple. Clearly, such sources are not expected to exist in the real world, and it is indeed remarkable that the observed variations follow even approximately the predicted variations. A more realistic model must take into account non constant expansion rates, the non conservation of magnetic flux, changes in γ , the finite acceleration time for the relativistic particles, and the initial finite dimensions. But these are relatively minor modifications, and the observed departures from the predictions of the simple model should not, as is sometimes done, be used to infer that the general class of expanding source models is not relevant to the variable source phenomena.

In the case of the non-instantaneous production of relativistic particles, the expected form of the variations may be determined by integrating equation 12.41 and the appropriate production function.

In the case where the initial volume of the source is not infinitely small, the initial spectrum is not opaque out to very short wavelengths, and the source is transparent at frequencies higher than some critical frequency ν_0 . In the transparent region of the spectrum the flux variations occur simultaneously and reflect only the rate of particle production and/or decay due to synchrotron and inverse Compton radiation.

The experimental determination of ν_0 may be used to estimate the initial size of the source. Characteristically $\nu_0 \sim 10-30$ GHz corresponding to initial

dimensions of about 10^{-4} arc seconds for $B \sim 10^{-4}$ Gauss. For typical radio sources with $0.1 < z < 1$, the initial size derived in this way is from 0.1 to 1 light year. This is roughly consistent with the direct determination of the angular sizes made by long baseline interferometry, but it must be emphasized that so far these measurements have not been made in sufficient detail to permit a detailed comparison, or to estimate from equation (12.21) the initial magnetic field.

In those sources where good data exists in the spectral region $\nu > \nu_0$, the observed variations occur simultaneously as expected from the model, and with equal amplitude indicating an initial spectral index $\alpha \sim 0$, or $\gamma \sim 1$ in good agreement with the value of γ derived from equations (12.46) and (12.45).

In the spectral region $\nu > \nu_0$, the observed flux variations depend on the total number of relativistic particles, their energy distribution, and the magnetic field. Thus observations in this part of the spectrum ^{more} closely reflects the rate of generation of relativistic particles than observations in the opaque part of the spectrum.

In some sources ν_0 occurs at relatively low frequencies of 1 or 2 GHz. This poses a serious problem, for the following reason. If variations occur on a time scale of the order of τ , then it is commonly assumed that the dimensions of the emitting region, l , is less than $c\tau$, since otherwise the light travel time from different parts of the source to the observer would "blur" any variations which occur. Using the distance obtained from the red shift, a limit to the angular size, θ , may be calculated; and from equation (12.22) an upper limit to the magnetic field strength is obtained.

For a typical quasar, such as 3C454.3, $\tau \sim 1$ year, $z \sim 1$, $\theta \lesssim 10^{-4}$ arc second, and $B \lesssim 10^{-5}$ Gauss. With such weak fields, the energy required in relativistic particles is very high and is $\sim 10^{58}$ ergs, and the repeated generation of such enormous energies in times of the order of one year or less is a formidable problem. Also the limit to the angular size deduced from the light travel time argument, often results in a peak brightness temperature which may exceed the expected maximum value of 10^{12} °K derived earlier. For these reasons it has been questioned by some whether or not in fact the quasars are at the large distances indicated by their red shifts, e.g. (Hoyle, Burbidge, and Sargent, 1966), or whether they do indeed radiate by the ordinary synchrotron process.

One way in which the theoretical brightness temperature limit may be exceeded, is if the relativistic electrons are radiating coherently. Stimulated emission or negative absorption is possible in opaque synchrotron sources, if the relativistic electrons are moving in a dispersive medium where the index of refraction is less than unity.

However, other than the seemingly excessive brightness temperature implied by some of the variable source observations, the expanding source model and the ordinary incoherent synchrotron process appears to be adequate to explain all of the observed phenomena.

Another way to explain the rapid variations was pointed out by Rees (1967), who showed that if the source is expanding at a velocity $v \sim c$, then the differential light travel time between the approaching and receding parts of the source can cause the illusion of an angular expansion rate corresponding to an apparent linear velocity $v > c$. In this case the angular size and peak

brightness temperature is smaller, and from equation (12.36) which depends on a high power of θ , the required energy is greatly reduced. However, there is a limit to the extent that the total energy requirements can be reduced, by this "super-light" expansion theory since as the particle energy is decreased when θ is increased, the magnetic energy is increased. The minimum value of the total energy occurs when the two are approximately equal, and for the typical quasar is $\sim 10^{55}$ ergs (e.g. van der Laan 1971).

Unfortunately, the variation in total intensity for the relativistically expanding source is very similar to that for the non relativistic model, so that they cannot be distinguished merely from observations of the intensity variations. The direct observation of the variations in angular size likewise do not distinguish between "super-light" velocities at cosmological distances, or non relativistic velocities in a "local" model for quasars.

An interesting variation on the expanding source model has been suggested by the Russian astrophysicists. Ozernoy and Sazinov (1969) who propose that two or more discrete components are "flying apart" at relativistic velocities, while at the same time expanding. Evidence for relativistic component velocities has been obtained from long baseline interferometer observations, but so far with the meagre data available at this time it has not been possible to uniquely distinguish between actual component motions, and properly phased intensity variations in stationary components.

It may be expected, however, that future observations of intensity variations as a function of wavelength, when combined with the direct observation of the variations in angular size will uniquely determine not only the dynamics and energetics of the radio outbursts, but will also specify the initial conditions of the outburst with sufficient accuracy to limit the range of theoretical

speculation concerning the source of energy and its conversion to relativistic particles. In particular, there must be increased emphasis on observations made at the shortest possible wavelengths, since these most nearly reflect the conditions during the time just following the outburst (eqn. 12.44).

12.5.9 Evolution of the Radio Sources - As a result of the discovery and continued observations of the intensity variations in radio galaxies and quasars, it is becoming increasingly clear that, on a cosmic time scale, the generation of particles occurs during very short times and is presumably the result of repeated violent events in the nuclei of galaxies and in quasars. This essentially precludes any statistical process such as Fermi acceleration whose time scale is measured in millions of years.

However, even aside from the question of the source of energy and its conversion to relativistic particles, is the problem of the formation and evolution of the extended radio sources. In particular, how are the clouds of relativistic particles confined, and what determines the characteristic double or multiple shape.

One particular problem has been the need to explain the extreme fine structure found in the outer parts of some extended sources such as Cygnus A, or the existence of sources with very high ratio of component separation to component size.

One interesting suggestion has been that rather than accelerate the relativistic particles themselves, the galactic nuclei and quasars expell massive coherent bodies which then explode at some distance from the origin and produce the particles in situ. But there is no experimental evidence that this occurs since all of the observed very compact opaque sources, and all of the variable sources are coincident with quasars or nuclei. Thus, it

appears that in each source the relativistic particles are in fact generated at a common point and diffuse out to form two or more extended clouds of particles. It has therefore been widely assumed that the individual components are confined by the intergalactic gas or intergalactic magnetic, although the required gas density or magnetic field strengths are uncomfortably large (e.g. Burbidge 1972). However, the possibility of sufficient gas being present in clusters, or being ejected from the galaxy itself does not seem unlikely.

which
A theory/is commonly discussed is the ram pressure model of De Young and Oxford (1967). The rather sharp outer boundaries found in many of the resolved sources lend support to this.

A model describing the evolution of double radio sources has been developed by Ryle and Longair (1967). They explain the ratio of observed intensity and separation from the parent object as the effect of the differential light travel time and other relativistic effects on two identical objects expanding with highly relativistic velocities.

12.6 SUMMARY

There is convincing quantitative evidence that all of the extragalactic radio sources radiate by the commonly accepted incoherent synchrotron process. This includes:

- 1) The shape of the spectra of the extended (transparent) sources are power law or dual power, and their detailed shape are in agreement with synchrotron models where the relativistic particles both gain and lose energy.
- 2) In the compact sources, the spectral peak occurs at shorter wavelengths in the smaller sources, as predicted by the synchrotron model, and the measured angular sizes are in good agreement with those estimated from the observed self absorption cutoff wavelength.

3) The maximum observed brightness temperature is $\sim 10^{12}$ °K, as is expected from an incoherent synchrotron source which is "cooled" by inverse Compton scattering.

4) The variations in intensity and polarization and its dependence on wavelength and time is in good agreement with that expected from an expanding cloud of relativistic particles.

The outstanding problems in the understanding of the radio galaxies and quasars are:

- 1) the source of energy and its conversion to relativistic particles;
- 2) the connection, if any, between the compact opaque sources and the extended transparent one;
- 3) the evolution of the extended sources.

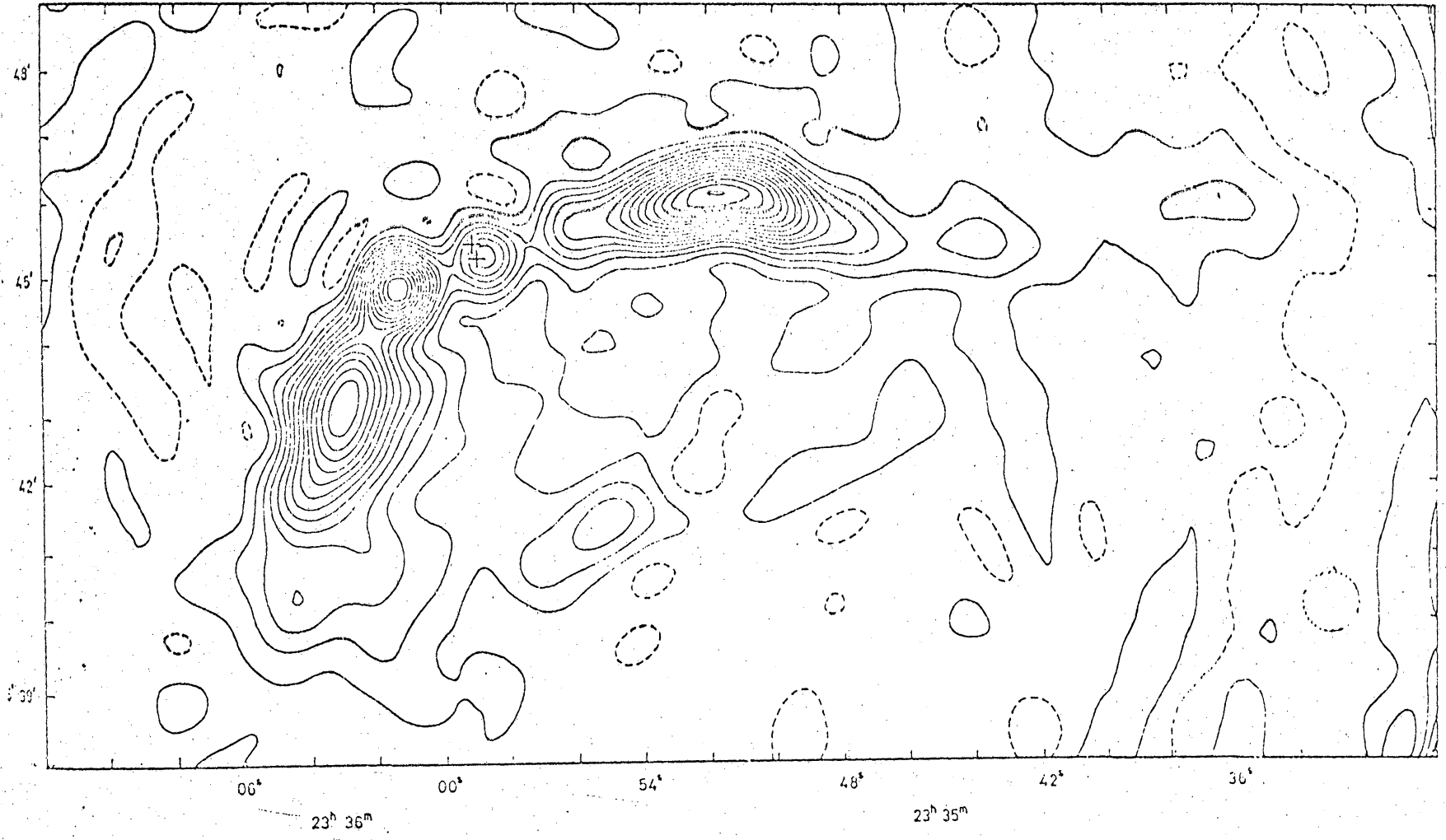
The third and possibly the second problem present challenging complex problems in magnetohydrodynamics and plasma physics, while the first may well require fundamentally new physics before it is understood.

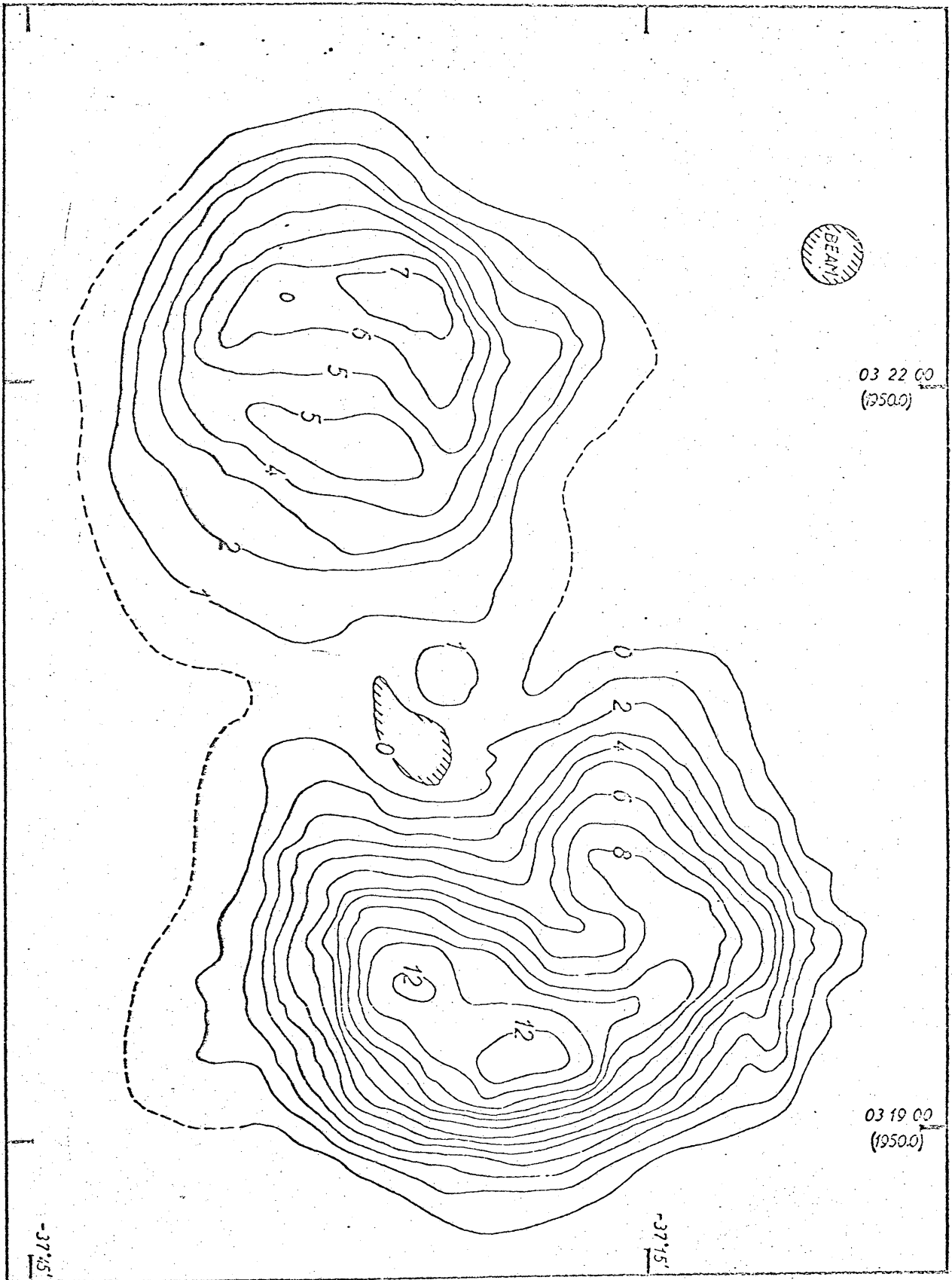
REFERENCES

- Aller, H. D., 1970, Astrophys. J. 161, 19.
- Baade, W. and Minkowski, R. 1954, Astrophys. J., 119, 206.
- Bennet, A. 1962, Mon. Roy. Astr. Soc. 68, 165.
- Bolton, J. G., Stanley, G., and Snee, B. 1949, Nature, 164, 101.
- Burbidge, G. 1972, I. A. U. Symp. No. 44, 492 (D. S. Evans, ed.) Springer-Verlag.
- Cohen, M. 1969, An. Rev. Astr. and Astroph., 7, 619.
- De Young, D. S. and Oxford, W. I., 1967, Nature, 216, 129.
- Dixon, R. S. 1970, Ap. J. Sup. 20, 1.
- Douglas, J. N. 1964, I. E. E. E. Trans. Mil. Electron, MIL-8, 173.
- Dixon, R., 1970, Ap. J. Suppl. 20, 1.
- Edge, D. O., Shakeshaft, J. R., McAdam, W. B., Baldwin, J. E., and Archer, S. 1960, Mem. Roy. Astr. Soc. 68, 37.
- Fomalont, E., 1969, Ap. J., 157, 1027.
- Ginzburg, V. L., 1951, Dokl. Akad. Nauk, U.S.S.R., 29, 418.
- Ginzburg, V. L., and Syrovetskii, S. I., 1964, The Origin of Cosmic Rays, Pergamon Press.
- Heeschen, D. S. 1960, P.A.S.P. 72, 368.
- Heeschen, D. S. 1966, Ap. J., 146, 517.
- Hoyle, F., Burbidge, G., and Sargent, W. L. 1969, Nature, 209, 751.
- MacDonald, G. H., Kenderdine, S., and Neville, A. C. 1968, M.N.R.A.S., 138, 259.
- Mathews, T., Morgan, W., and Schmidt, M. 1964, Ap. J., 140, 35.
- Miley, G. K., and Wade, C. M., 1971, Astrophys. Let., 8, 11.
- Morgan, W. W., 1972, I.A.U. Symposium No. 44, 97 (D. S. Evans, ed.) Springer-Verlaag.

- Ozernog, L. M. and Sazonov, V. N., 1969, Astrophys. and Space Sci., 3, 395.
- Rees, M. 1967, Mon. Not. Roy. Astron. Soc., 135, 345.
- Rogstad, P. and Ekers, R., 1969, Astrophys. J., 157, 481.
- Ryle, M. and Longair, M. 1967, Mon. Not. Roy. Astr. Soc., 136, 123.
- Scheuer, P. A. G. 1962, Austr. J. Phys. 15, 333.
- Shklovsky, I. S. 1952, Astr. Zhur. U.S.S.R. 29, 418.
- van der Laan, 1966, Nature, 211, 1131.
- van der Laan, 1971, Semaine de Etude,
- von Hoerner, S., 1964, Astrophys. J., 140, 65.

1407 MHz





BEANS

03 22 00
(250.0)

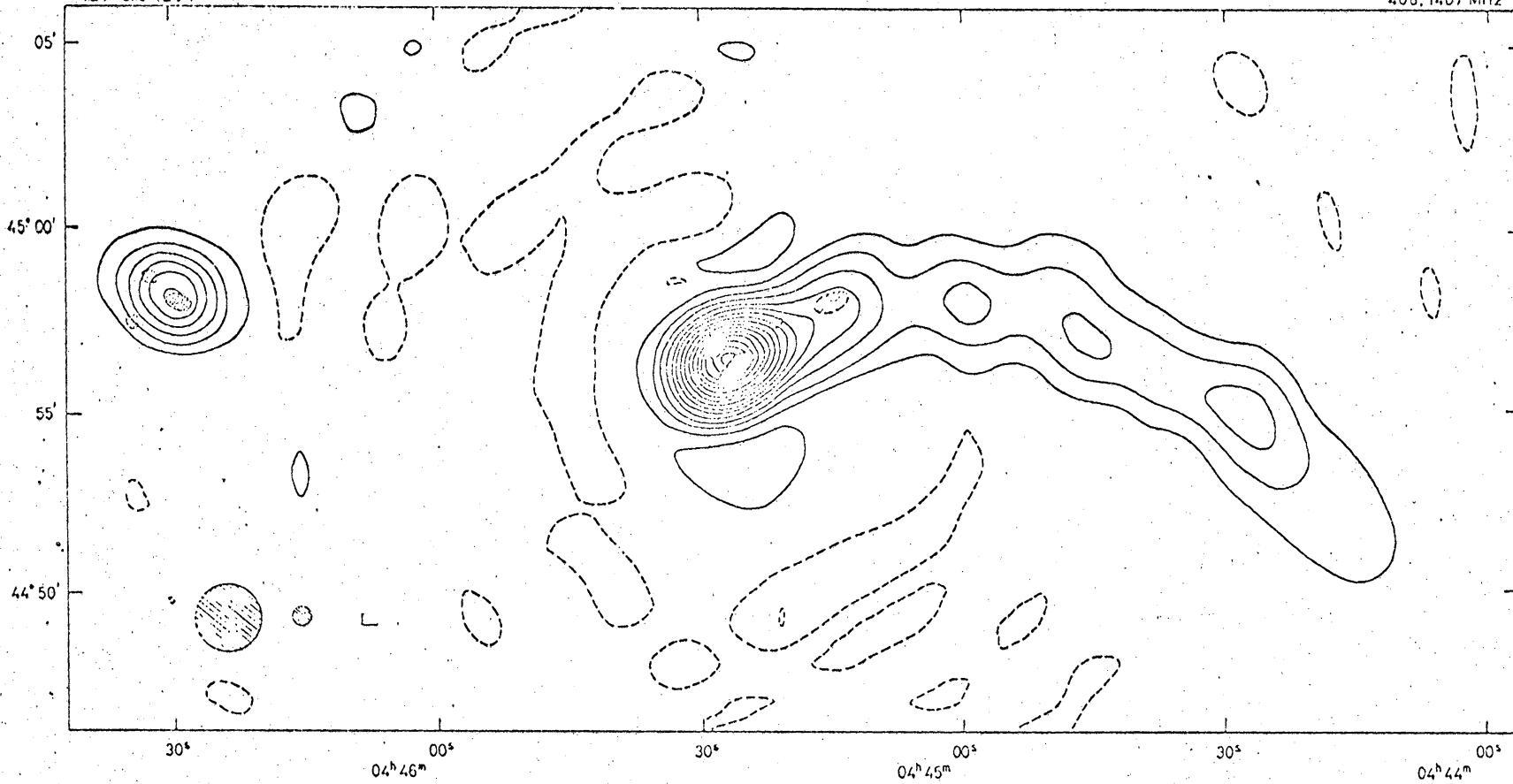
03 19 00
(1950.0)

-37'15'

-37'15'

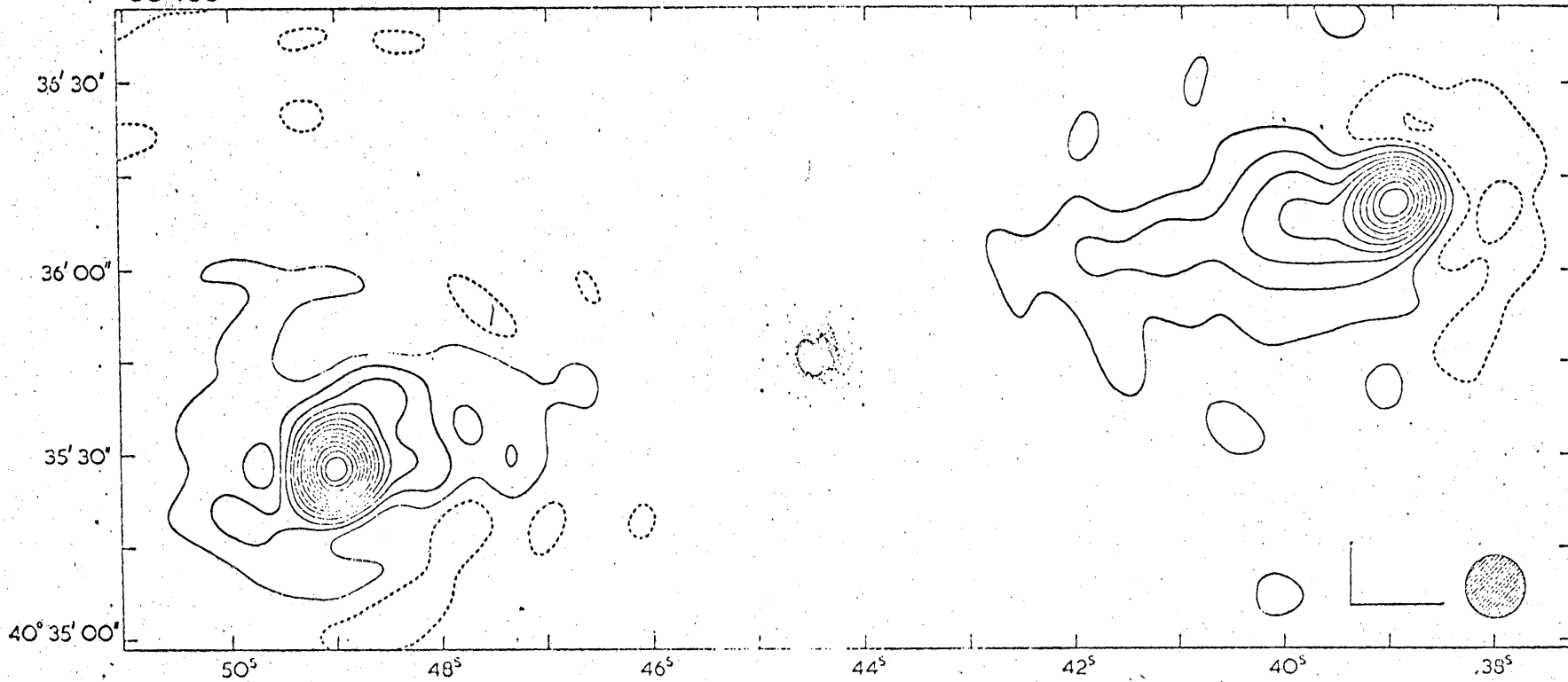
129 and 129.1

408, 14.07 MHz



3C 405

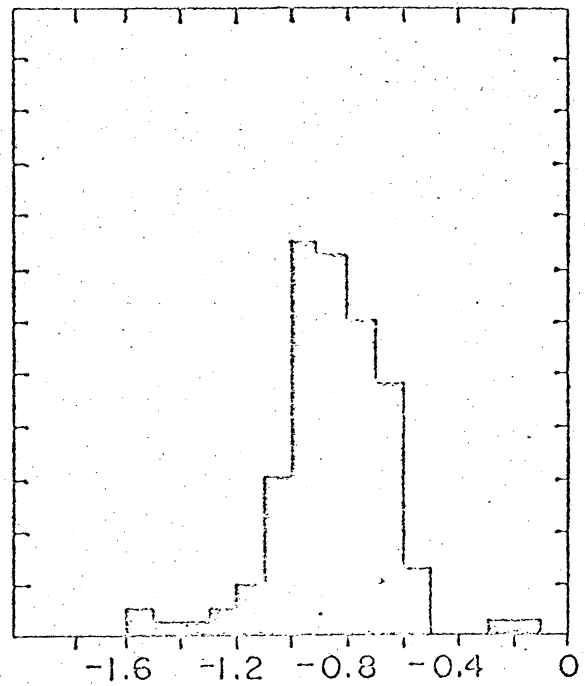
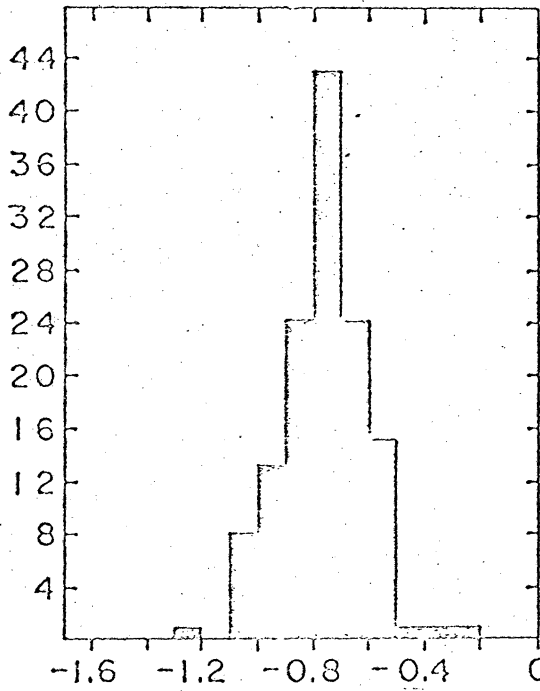
4.995GHz



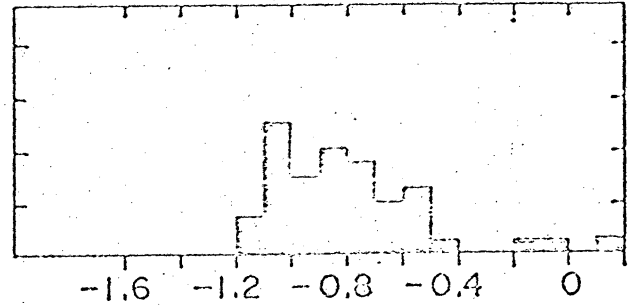
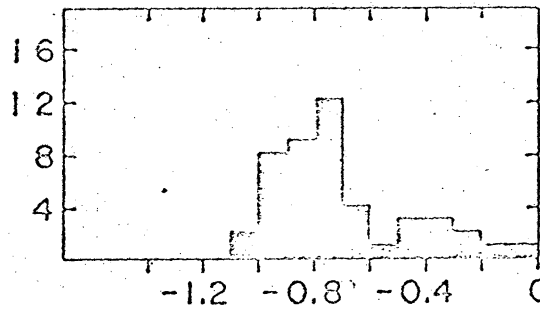
38-750 MHz

750-5000 MHz

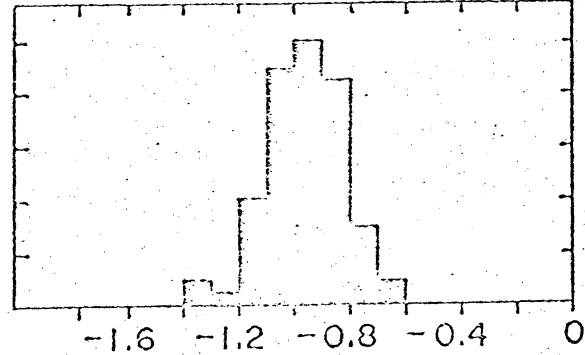
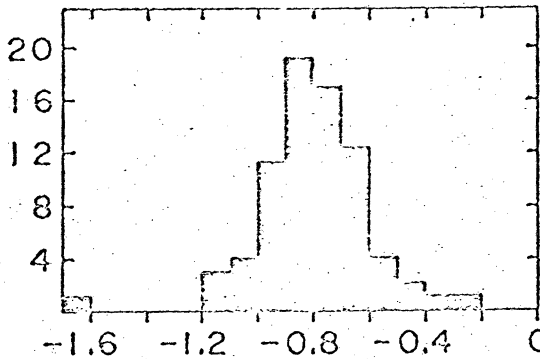
GALAXIES

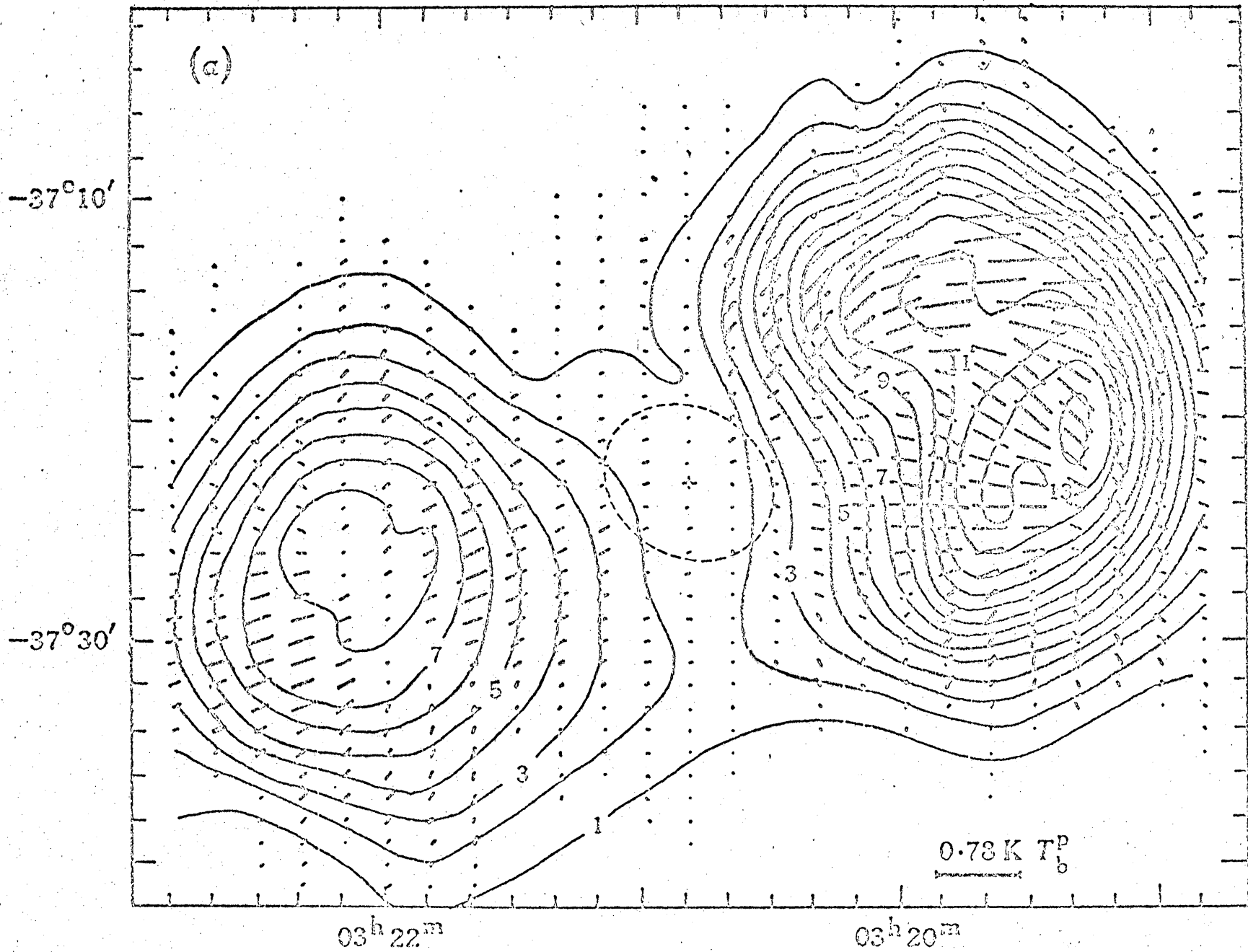


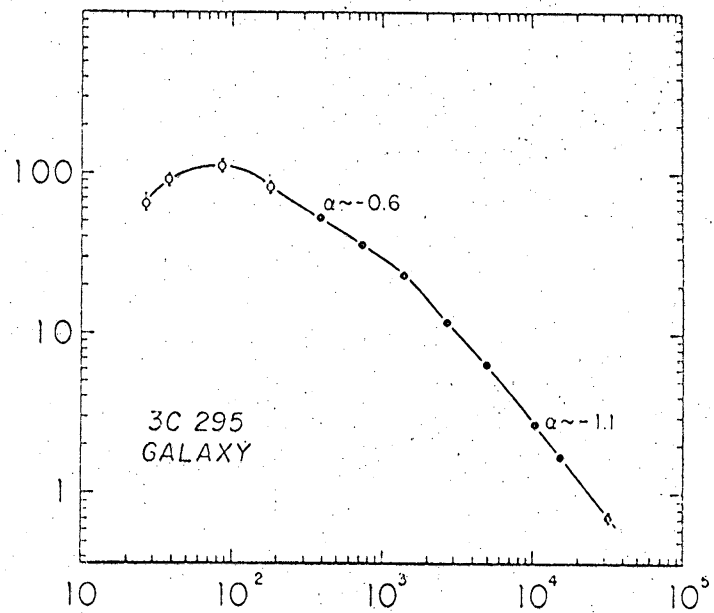
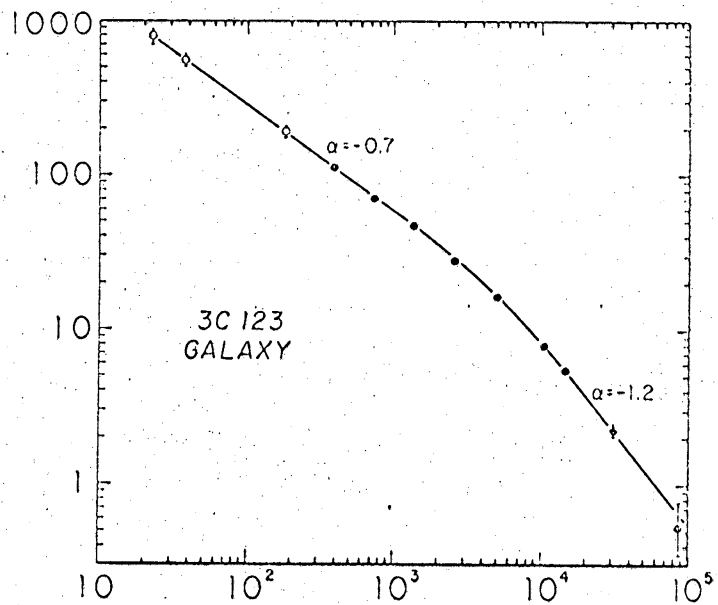
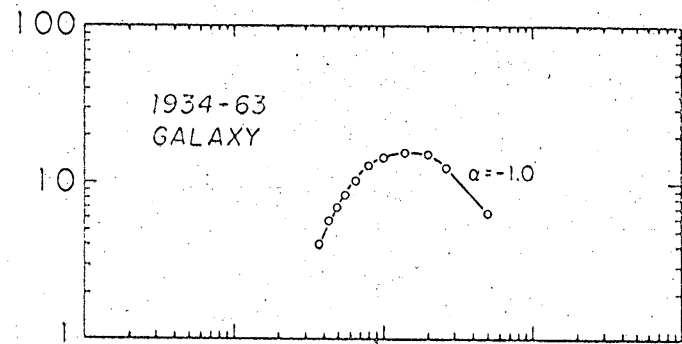
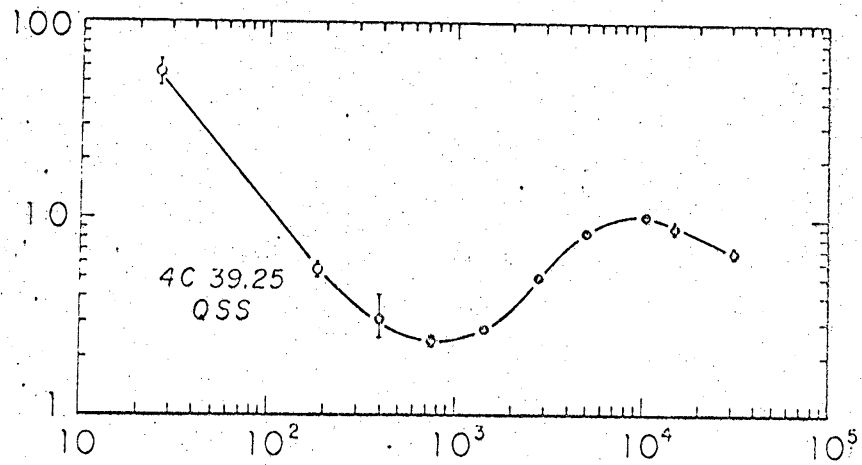
QSS

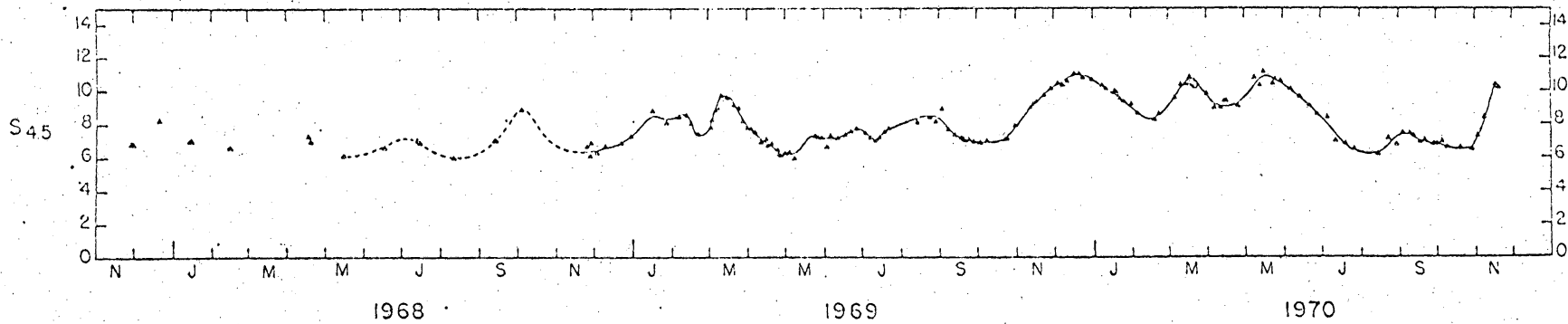
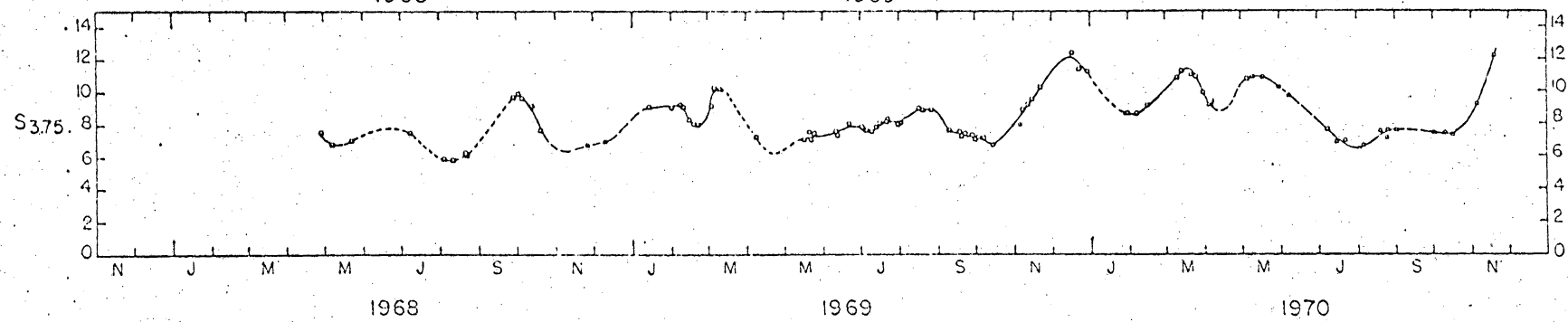
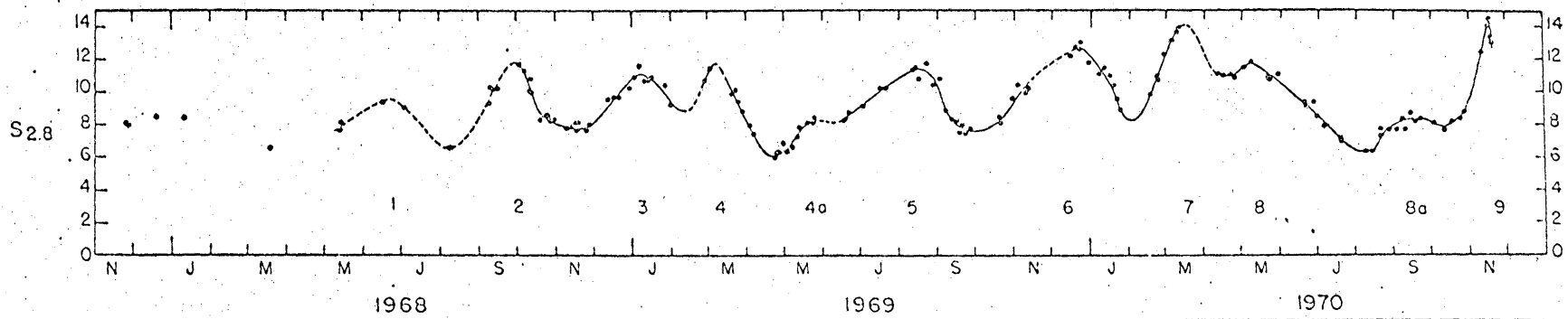


UNIDENTIFIED SOURCES









LUMINOSITY VS BRIGHTNESS

$$S_{1400} > 4.0 \text{ f.u.}$$

